Screening of genes specifically activated in the pancreatic juice ductal cells from the patients with pancreatic ductal carcinoma

Koji Yoshida,[1,6] Shuichi Ueno,[1,2] Toshiyasu Iwao,[6] Souichirou Yamasaki,[7] Akira Tsuchida,[7] Ken Ohmine,[1,3] Ruri Ohki,[1,2] Young Lim Choi,[1] Koji Koinuma,[1,4] Tomoaki Wada,[1,5] Jun Ota,[1] Yoshihiro Yamashita,[1] Kazuaki Chayama,[7] Kazuhiro Sato[6] and Hiroyuki Mano[1,8]

Divisions of [1]Functional Genomics, [2]Cardiology and [3]Hematology, Departments of [4]Surgery and [5]Gynecology, Jichi Medical School, 3311-1 Yakushiji, Kawachi-gun, Tochigi 329-0498, [6]Gastroenterological Center, Aizu Central Hospital, 1-1 Tsurugamachi, Aizuwakamatsu-shi, Fukushima 956-8611 and [7]First Department of Internal Medicine, Faculty of Medicine, Hiroshima University, 1-2-3 Kasumi, Hiroshima-shi, Hiroshima 734-8551

(Received November 8, 2002/Revised January 7, 2003/Accepted January 14, 2003)

Pancreatic ductal carcinoma (PDC) is one of the most intractable human malignancies. Surgical resection of PDC at curable stages is hampered by a lack of sensitive and reliable detection methods. Given that DNA microarray analysis allows the expression of thousands of genes to be monitored simultaneously, it offers a potentially suitable approach to the identification of molecular markers for the clinical diagnosis of PDC. However, a simple comparison between the transcriptomes of normal and cancerous pancreatic tissue is likely to yield misleading pseudopositive data that reflect mainly the different cellular compositions of the specimens. Indeed, a microarray comparison of normal and cancerous tissue identified the *INSULIN* gene as one of the genes whose expression was most specific to normal tissue. To eliminate such a "population-shift" effect, the pancreatic ductal epithelial cells were purified by MUC1-based affinity chromatography from pancreatic juice isolated from both healthy individuals and PDC patients. Analysis of these background-matched samples with DNA microarrays representing 3456 human genes resulted in the identification of candidate genes for PDC-specific markers, including those for *AC133* and carcinoembryonic antigen-related cell adhesion molecule 7 (*CEACAM7*). Specific expression of these genes in the ductal cells of the patients with PDC was confirmed by quantitative real-time polymerase chain reaction analysis. Microarray analysis with purified pancreatic ductal cells has thus provided a basis for the development of a sensitive method for the detection of PDC that relies on pancreatic juice, which is routinely obtained in the clinical setting. (Cancer Sci 2003; 94: 263–270)

Pancreatic carcinoma remains the most intractable disorder among gastroenterological malignancies, with a 5-year survival rate of <5%.[1,2] More than 90% of pancreatic carcinomas are adenocarcinomas of ductal cell origin. In part because of the lack of disease-specific symptoms, individuals at an early stage of pancreatic carcinoma are rarely detected, and the probability of tumors being suitable for surgical resection at the time of discovery is low (10 to 20%). Several improvements in imaging analysis of pancreatic structure have recently been achieved, including endoscopic retrograde cholangiopancreatography (ERCP), magnetic resonance cholangiopancreatography (MRCP), and endoscopic ultrasound examination.[3] However, even with these procedures, it often remains difficult to distinguish pancreatic carcinoma from other disorders such as chronic pancreatitis. Furthermore, these methods usually detect only those pancreatic tumors with a diameter of >5 mm. Given the low 5-year survival rate (20 to 30%) even of individuals with small, resectable tumors, the sensitivity of current technologies is not sufficient to allow detection of pancreatic carcinoma at curable early stages. A cure for this disorder will thus depend on development of an approach that is able to detect tumors at an early stage of carcinogenesis.

Pancreatic ductal carcinoma (PDC) arises from epithelial cells of the pancreatic duct. Carcinoma cells of individuals with this condition are thus shed into pancreatic juice. Analysis of these cells appears a promising approach to the development of a sensitive method for the diagnosis of pancreatic carcinoma. Indeed, molecular biological analysis of these tumor cells has revealed a variety of genetic alterations associated with the pathogenesis of pancreatic carcinoma. Activating point mutations of the K-*RAS* proto-oncogene have thus been identified in >80% of individuals with pancreatic carcinoma,[4] and inactivation of the *TP53* tumor suppressor gene has been detected at a similar frequency.[5] Other mutations have been identified in the genes for p16, DPC4, and DCC.[6–8] However, K-*RAS* mutations are also evident at a relatively high frequency in nonmalignant pancreatic disorders.[9] To date, no molecular markers proven to be specific to carcinoma cells of pancreatic ductal origin have been identified.

DNA microarray analysis allows the simultaneous monitoring of the expression of thousands of genes[10,11] and is therefore a potentially suitable approach to identify PDC-specific genes. The high throughput of this methodology also may be disadvantageous, however. Without careful selection of samples for analysis or data normalization procedures, DNA microarray experiments yield large numbers of pseudopositive and pseudonegative results. In the case of PDC, a simple comparison of pancreatic tissue obtained from individuals with nonmalignant or cancerous conditions would likely not prove informative. Most normal pancreatic tissue comprises exocrine and endocrine cells, with ductal structures constituting only a small proportion of the total volume of the normal pancreas. In contrast, cancerous pancreatic tissue consists mostly of tumor cells that arise from ductal epithelial cells. A comparison between nonmalignant and cancerous tissue would thus likely identify differences between the gene expression profiles of exocrine and endocrine cells and that of tumor cells of ductal cell origin, rather than differences between those of normal and transformed cells of the same origin.

We now show that such a tissue comparison for PDC is indeed uninformative with regard to the identification of tumor-specific genes. To avoid this pitfall, we therefore adopted the strategy of "background-matched population (BAMP) screening,"[12] in which the sample characteristics are matched as closely as possible, with the exception of the feature of interest (in this case, transformation), before microarray analysis. To achieve this goal, we purified pancreatic carcinoma cells and normal ductal cells from pancreatic juice with the use of affinity chromatography based on the shared surface marker MUC1.

[8]To whom correspondence and reprint requests should be addressed.
E-mail: hmano@jichi.ac.jp

Comparison of these two cell preparations by DNA microarray analysis revealed a group of genes that are potential molecular markers specific to PDC.

Materials and Methods

Preparation of pancreatic ductal cells. The study subjects comprised individuals who were subjected to ERCP and to the collection of pancreatic juice for cytological examination and who gave informed consent. The study was approved by the institutional review boards of Jichi Medical School, Aizu Central Hospital and Hiroshima University. Diagnosis of patients was confirmed on the basis both of the combination of results obtained by ERCP, cytological examination of pancreatic juice, abdominal computed tomography, and measurement of the serum concentration of CA19-9, as well as of follow-up observations. About one-third of each pancreatic juice specimen was used to purify $MUC1^+$ ductal cells. Cells were collected from the pancreatic juice by centrifugation and resuspended in 1 ml of MACS binding buffer [150 m*M* NaCl, 20 m*M* sodium phosphate (pH 7.4), 3% fetal bovine serum, 2 m*M* EDTA]. The cells were then incubated for 30 min at 4°C with 0.5 μg of mouse monoclonal antibodies to MUC1 (Novocastra Laboratories, Newcastle upon Tyne, UK), washed with MACS binding buffer, and mixed with MACS MicroBeads conjugated with antibodies to mouse immunoglobulin G (Miltenyi Biotec, Auburn, CA). The resulting mixture was subjected to chromatography on miniMACS magnetic cell separation columns (Miltenyi Biotec). The eluted $MUC1^+$ cells were divided into aliquots and stored at −80°C. Portions of the unfractionated cells as well as of the isolated $MUC1^+$ cells of each individual were stained with Wright-Giemsa solution to examine the purity of the ductal cell-enriched fractions.

Isolation of RNA and microarray analysis. Total RNA was extracted from the $MUC1^+$ cell preparations with the use of RNAzol B (Tel-Test, Friendswood, TX), and portions (20 μg) of the resulting preparations were subjected to amplification of mRNA with T7 RNA polymerase as described.[13] Biotin-labeled cRNA was synthesized from the amplified RNA (2 μg) with the use of the ExpressChip labeling system (Mergen, San Leandro, CA) and was then subjected to hybridization with microarrays (HO-1 to -3, Mergen) that contain oligonucleotides corresponding to a total of 3456 human genes (for a list of the genes, see http://www.mergen-ltd.com). The microarrays were then incubated consecutively with streptavidin, antibodies to streptavidin, and Cy3-conjugated secondary antibodies (Mergen). Detection and digitization of hybridization signals were performed with a GMS 418 array scanner (Affymetrix, Santa Clara, CA). The fluorescence intensity for each gene was normalized relative to the median fluorescence value for all genes in each array hybridization. Statistical analysis of the data was performed with GeneSpring 5.0 software (Silicon Genetics, Redwood, CA).

Real-time polymerase chain reaction (PCR) analysis. Portions of unamplified cDNA were subjected to the PCR with SYBR Green PCR Core Reagents (PE Applied Biosystems, Foster City, CA). Incorporation of the SYBR Green dye into the PCR products was monitored in real time with an ABI PRISM 7700 sequence detection system (PE Applied Biosystems), thereby allowing determination of the threshold cycle (C_T) at which exponential amplification of PCR products begins. The C_T values for cDNAs corresponding to the *β-actin* gene and target genes were used to calculate the abundance of the target transcripts relative to that of β-actin mRNA. The oligonucleotide primers for PCR were as follows: 5′-CCATCATGAAGTGTGACGTGG-3′ and 5′-GTCCGCCTAGAAGCATTTGCG-3′ for β-actin cDNA, 5′-TCCTGGGACTGTGACTTTCA-3′ and 5′-CTTTTGGTCCAGACCCTCAA-3′ for small ubiquitin-like modifier (SUMO) 1 cDNA, 5′-CCATCATGAAGTGTGACGTGG-3′ and 5′-GTCCGCCTAGAAGCATTTGCG-3′ for carcinoembryonic antigen-related cell adhesion molecule (CEACAM) 7 cDNA, and 5′-GAGACTCAGAACACAACCTACCTG-3′ and 5′-AGCCAGTACTCCAATCATGATGCT-3′ for AC133 cDNA.

Results

Purification of ductal cells from pancreatic juice. Pancreatic juice contains various types of cells, including pancreatic ductal cells, erythrocytes, neutrophils, and lymphocytes (Fig. 1A). Given that the proportions of these cellular components of pancreatic juice vary markedly among individuals, the purification of ductal cells is required for reliable comparison of gene expression profiles. Normal and cancerous pancreatic ductal cells express various mucins. Among those, MUC1 is known to be expressed in both normal and cancerous ductal cells, whereas others, such as MUC3 and MUC5, are differentially expressed in a disease-dependent manner.[14, 15] We therefore developed an affinity purification approach for pancreatic ductal cells based on MUC1 as a common surface marker. Cells specifically eluted from a magnetic bead separation column exhibited an epithelial cell-like morphology (Fig. 1B).

Previous attempts to identify genes whose expression is specific to PDC have often compared the gene expression profiles of normal and cancerous pancreatic tissues.[16] However, such an approach may result in the identification of genes that are differentially expressed between exocrine-endocrine cells and ductal cells. To directly examine if this is the case, we first compared the transcriptomes of surgically resected normal (n=1) and cancerous (n=2) pancreatic tissues by oligonucleotide microarray analysis. The digitized expression intensities for the 3456 human genes examined were normalized relative to the median expression level of all genes in each hybridization; in the case of the cancer tissue, the average expression value for each gene in the two specimens was further calculated. The expression level of every gene was then compared between the normal and cancerous tissues. One of the genes whose expression was most specific for the normal pancreatic tissue was that for insulin; its expression level in normal tissue was 6.869 arbitrary units (U) whereas the averaged value in the cancerous tissues was 1.22 U. Given that insulin is expressed only in islets of Langerhans, this result likely reflects the difference in the proportion of endocrine cells between the samples, not a difference in the number of *INSULIN* gene transcripts per cell between normal and cancer cells.

We next prepared $MUC1^+$ ductal cells from two individuals who were diagnosed as negative for PDC. Microarray analysis of these cells and comparison of the resulting data with those obtained with normal pancreatic tissue also identified the *INSULIN* gene as one of the most differentially expressed genes between the two types of sample; the averaged *INSULIN* expression level in the ductal specimens was 0.495 U, while that in the normal tissue section was 6.869 U.

Given that the proportion of cells of ductal origin would be expected to be markedly increased in cancerous pancreatic tissue compared with that in normal pancreatic tissue, these data support our expectation that a simple comparison of surgically resected specimens of normal and cancerous tissues from the pancreas is not a suitable approach to identify transformation-related genes of the ductal cell lineage.

Gene expression profiles of ductal cells obtained from pancreatic juice. An ideal strategy to identify potential molecular markers specific to PDC would be to compare the transcriptomes of ductal cells isolated from the pancreatic juice of healthy individuals and cancer patients. Any difference identified between the transcriptomes by such screening would thus likely reflect the transformation process, given that both of the samples would be of the same cellular origin. Furthermore, from the

Fig. 1. Purification of pancreatic duct cells from pancreatic juice. (A) Cells isolated by centrifugation from the pancreatic juice of an individual with PDC were subjected to Wright-Giemsa staining (magnification, 100×). In addition to cells of epithelial origin, both red blood cells and neutrophils (arrowheads) are apparent. (B) Cells separated from the pancreatic juice of the same individual with PDC were subjected to chromatography on a MUC1-based affinity column. Cells specifically eluted from the column were then subjected to Wright-Giemsa staining (magnification, 200×). Some of the eluted cells exhibited a cancer-specific aberrant phenotype (large nuclei with fine chromatin structure).

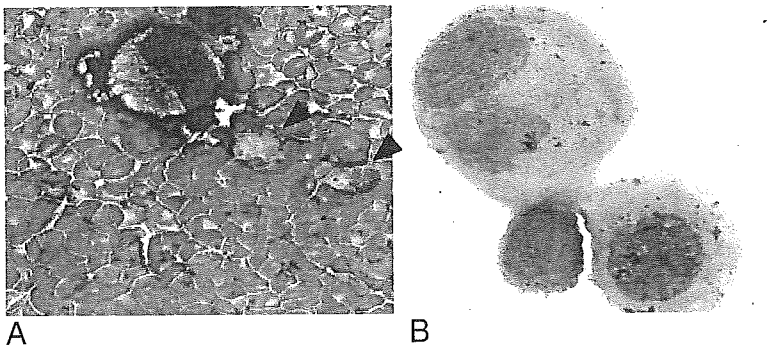

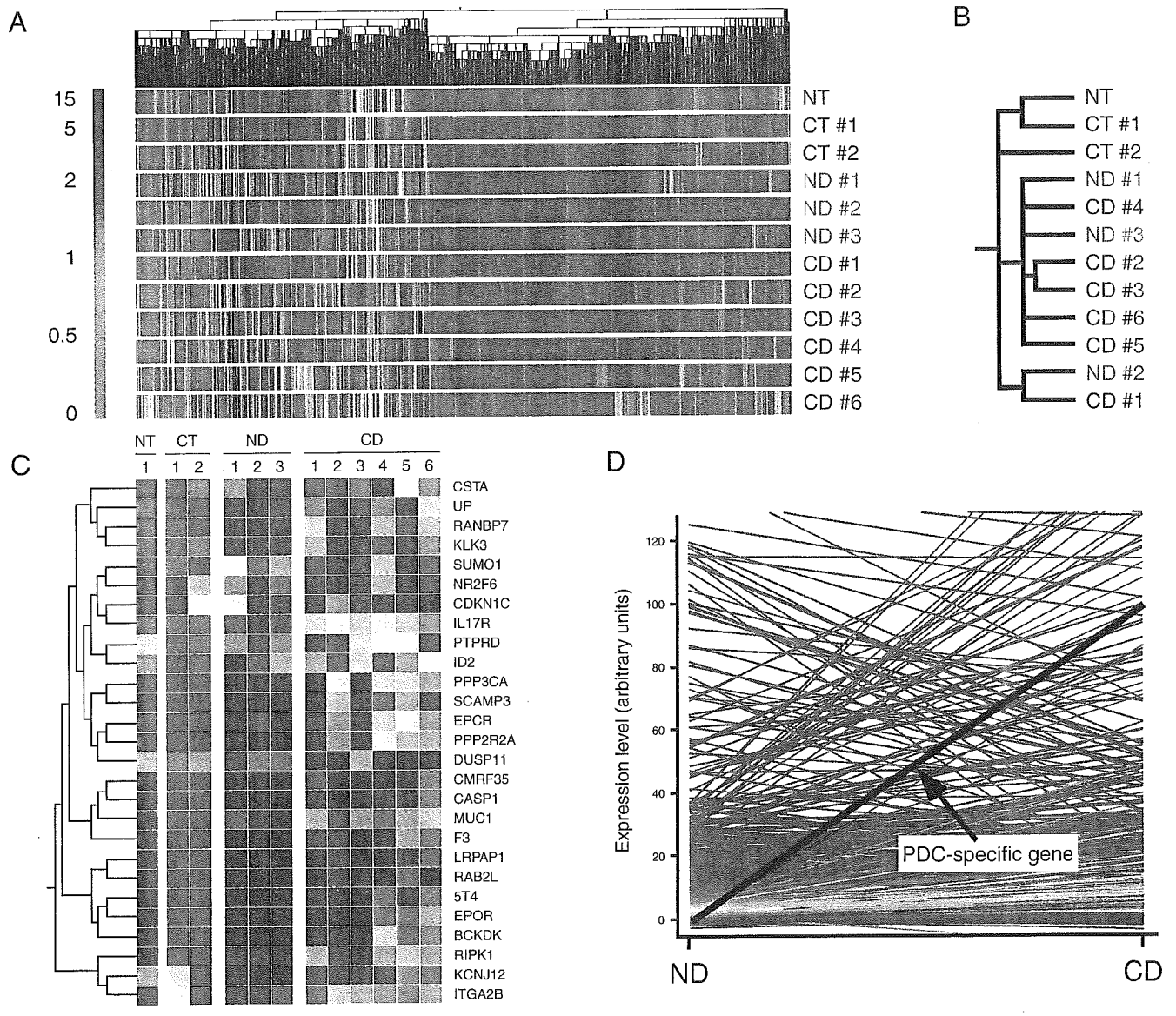

Fig. 2. (A) Hierarchical clustering of 3456 genes based on their expression profiles in pancreatic tissue specimens from one normal individual (NT) and two PDC patients (CT #1 and #2) as well as in MUC1$^+$ ductal cells obtained from three normal individuals (ND #1–3) and six cancer patients (CD #1–6). Each column represents a single gene on the microarray, and each row corresponds to a different subject. The normalized fluorescence intensity for each gene is shown color-coded as indicated at the left. (B) Two-way clustering analysis of the transcriptomes shown in (A) was performed to assess statistically the similarity among the samples from the different subjects and to generate a subject dendrogram. (C) Hierarchical clustering of the "disease-dependent" genes. Expression intensities are shown color-coded according to the scale in (A). Gene symbols are indicated at the right. (D) Comparison of the expression levels of 3456 human genes between normal and cancerous ductal cells. The normalized value for the expression level of each gene was averaged for three normal ductal cell specimens and was compared with the corresponding value obtained with six cancerous ductal cell samples. Each line corresponds to a single gene on the array and is presented color-coded according to the expression level in the normal tissue according to the scale shown in (A). The line for a hypothetical "PDC-specific gene" is indicated in blue.

point of view of clinical application, this BAMP screening approach also appears desirable. The identification of *bona fide* cancer-specific genes would thus allow development of a sensitive method for the diagnosis of PDC based on reverse transcription and PCR (RT-PCR) analysis of cells isolated from pancreatic juice, which can be obtained during the ERCP procedure.

In an attempt to realize this goal, we compared the expression profiles of 3456 genes among one specimen of normal pancreatic tissue (NT), two specimens of cancerous pancreatic tissue (CT #1 and #2), three normal ductal cell preparations (ND #1 to #3), and six ductal cell preparations obtained from PDC patients (CD #1 to #6). The clinical information is summarized in Table 1 for the PDC patients who provided pancreatic juice. All of the ductal cell preparations of the CD patients were cytologically diagnosed to contain "class IV" cells, the proportion of which is also shown in the table. Since all CD patients already had tumor invasion into either the splenic artery or the portal vein as judged by angiography, none of them was suitable for surgical operation. Therefore, we do not have any pathological data of pancreatic tissues for any of the PDC patients in Table 1. All CD patients died within 12 months after diagnostic procedures.

Table 1. Clinical characteristics of the patients with PDC

Patient ID	Sex	Age (yr)	Liver metastasis	SA or PV invasion	Proportion of class IV cells (%)
CD #1	M	71	–	+	6.4
CD #2	F	61	–	+	45.3
CD #3	F	82	–	+	4.6
CD #4	F	68	+	+	4.2
CD #5	F	73	+	+	12.6
CD #6	F	71	–	+	33.4

M, male; F, female; yr, year; SA, splenic artery; PV, portal vein.

The ND #1–3 individuals were subjected to ERCP procedure due to a slight elevation in blood amylase level or to the echographic finding of dilation of the pancreatic duct. However, ERCP examination could detect no anomaly in their ductal structure. These individuals were also negative for PDC in cytological analysis of pancreatic juice, and are still healthy after >12 months of observation.

The gene expression profiles of each sample were subjected to clustering analysis in order to generate a dendrogram, or "gene tree," in which genes with similar expression profiles are clustered together (Fig. 2A). Such analysis revealed that the patterns of gene expression of ND #1 and #3 were similar to those of CD #2 to #6. However, despite this overall similarity, significant differences between these two types of sample were apparent, some of which might reflect the carcinogenic process.

To statistically analyze the similarity of transcriptomes among the samples, we performed two-way clustering analysis[17] to generate a "subject tree," in which samples with similar transcriptomes are grouped together (Fig. 2B). All ductal cell samples (ND and CD) were clustered in two major branches, separated from the tissue samples, which indicates that the transcriptomes of the cancerous ductal cells were more similar to those of the normal ductal cells than they were to those of the cancer tissue specimens. The transcriptomes of ductal cell samples from cancer patients #2 and #3 exhibited the greatest similarity.

Potential molecular markers for PDC. Our data suggest that a direct comparison between normal and cancerous ductal cells would be a suitable means to efficiently identify the PDC-specific

Table 2. Expression level of the disease-dependent genes

Gene symbol	GenBank #	NT	CT #1	CT #2	ND #1	ND #2	ND #3	CD #1	CD #2	CD #3	CD #4	CD #5	CD #6
DUSP11	AF023917	3.833	0.924	1.387	0.358	1.056	5.102	−0.056	22.841	3.826	22.211	30.331	15.227
KCNJ12	L36069	4.157	2.096	10.149	−0.166	−0.422	−0.284	0.356	0.169	0.087	−0.164	1.106	0.168
ITGA2B	J02764	7.498	3.165	9.311	0.322	0.261	0.773	0.730	2.072	1.668	1.284	1.000	1.340
CSTA	X05978	−0.962	−0.905	0.638	1.100	−1.487	−0.366	12.865	7.687	5.928	−0.164	2.528	0.809
UP	X90858	0.637	−0.182	−0.378	−0.447	−0.092	0.062	0.977	0.021	0.209	1.000	0.056	2.205
SUMO1	U61397	−1.043	0.557	−0.933	2.703	0.841	1.618	0.196	10.385	11.219	1.952	16.324	8.469
PPP3CA	M29550	−0.511	−0.926	−0.938	−0.747	−1.191	−0.214	−1.587	2.656	−0.427	2.267	3.231	1.701
PTPRD	L38929	2.149	0.333	0.694	1.310	0.149	1.140	−0.104	7.369	3.223	2.997	2.793	6.908
LRPAP1	M63959	−0.387	−0.790	−0.541	−0.805	−0.595	−0.265	−0.339	0.399	−0.352	−0.291	0.062	0.759
RANBP7	AF098799	0.351	0.256	−0.741	−0.389	−0.303	0.018	3.466	0.142	−0.395	1.834	0.673	1.968
EPCR	L35545	0.440	−0.558	−0.393	−0.483	0.581	−0.050	0.194	1.277	0.125	3.373	2.891	1.384
RAB2L	U68142	−0.638	−1.144	−0.829	−0.856	−1.214	−1.341	−1.507	0.226	−0.848	−0.014	0.803	−0.100
5T4	Z29083	−0.412	−0.913	−0.338	−0.710	−0.724	−0.104	0.221	−0.136	−0.492	0.897	0.102	1.044
PPP2R2A	M64929	0.501	−0.858	−0.442	−0.501	−0.376	−0.194	−0.448	1.272	−0.380	2.474	3.584	1.677
EPOR	M34986	−0.008	−1.112	−0.744	−0.692	−0.671	−0.143	−0.093	−0.246	−0.438	0.857	0.898	1.727
BCKDK	AF026548	−0.202	−1.266	−0.713	−1.002	−0.900	−0.260	−0.876	0.129	−0.256	2.188	0.852	1.089
ID2	M97796	1.247	−0.076	0.389	−0.531	0.572	1.695	1.721	6.419	3.258	0.659	4.139	2.867
NR2F6	X12794	−1.279	−0.502	1.768	1.270	−0.713	5.963	−0.921	20.658	30.415	1.672	28.746	23.043
RIPK1	U50062	0.095	8.471	−0.001	0.422	0.367	0.190	1.819	0.450	0.032	1.404	2.050	1.607
KLK3	M26663	0.384	0.192	0.780	−0.038	−0.095	−0.066	1.653	0.276	0.041	0.556	0.277	0.937
CMRF35	X66171	−1.406	−0.541	−0.824	−0.171	−0.327	−0.129	0.521	0.076	−0.024	−0.190	0.076	0.579
SCAMP3	AF005039	−0.362	−1.002	−0.628	−0.493	−1.060	−0.270	−0.734	1.936	0.099	0.781	1.827	0.410
CASP1	U13698	−0.808	−0.132	−1.027	0.025	−0.113	−0.070	0.300	−0.009	0.123	0.279	0.187	0.726
F3	J02931	−1.096	−0.562	−0.286	−0.261	−0.607	−0.325	0.364	0.349	0.038	−0.276	1.530	0.388
MUC1	J05581	−2.454	0.398	−0.759	0.771	0.330	0.070	1.775	0.534	1.387	0.863	1.642	1.925
CDKN1C	U22398	0.057	−0.434	3.034	2.572	−1.003	−0.375	−0.138	4.131	10.992	9.788	8.131	11.543
IL17R	U58917	0.707	0.647	0.432	0.765	−0.138	0.263	2.322	2.692	3.360	2.452	3.319	5.122

Expression level of the "disease-dependent" genes is shown in arbitrary units (U). Gene symbol as well as GenBank accession number (#) is indicated for each gene.

transcriptome changes while keeping pseudo-positive data minimum. To identify *bona fide* PDC-specific genes from the array data, we here took two approaches.

First, expression levels of 3456 genes were compared between ND and CD sample types by Welch ANOVA test. Twenty-seven genes were thus identified, whose expression levels were statistically significantly different in the two types ($P<0.05$). A dendrogram of such disease-dependent genes is shown in Fig. 2C. Many genes in the list, including those for *SUMO1* (GenBank accession no. U61397) and dual specificity phosphatase (*DUSP*) *11* (GenBank accession no. AF023917), were inducibly expressed in PDC cells. Like ubiquitin, SUMO1 functions as a protein "tag," transfer of which is mediated by a SUMO E_3 ligase. In contrast to ubiquitin, however, modification with SUMO1 not only drives the substrates into a proteasome pathway, but has a pleiotropic effect on the substrates, such as protection against proteolysis, induction of apoptosis, and regulation of substrate function.[18,19] The *in vivo* role of SUMO1 is thus likely to be context-dependent, and it is an interesting question whether increased SUMO-tagging has a transforming or anti-apoptotic activity in PDC cells. The array data for these "disease-dependent" genes are shown in detail in Table 2. These genes would be good candidates to be included in custom-made DNA microarrays specialized for the diagnosis of PDC.

However, there is a caveat that this type of comparison may isolate genes whose absolute expression levels may be negligibly low. Actually, fifteen out of twenty-seven genes in Table 2 did not have expression levels of more than 3.0 U in any ductal cell preparation.

Therefore, we also tried another approach to select PDC-specific genes. The mean expression value of each gene was calculated for the ND or CD sample type, and the differences in the resulting values are represented in Fig. 2D. To identify genes whose mean expression values were induced only in the cancerous ductal cells, with the use of GeneSpring software, we searched for genes whose expression profiles were statistically similar, with a minimum correlation of 0.99, to that of a hypothetical "PDC-specific gene" (blue line in Fig. 2D) that exhibits a mean expression level of 0.0 U in the ND group and 100.0 U in the CD group. Taking the 188 genes thus identified, we then applied the criteria that the gene expression value should be (1) <3.0 U in all NT/ND samples and (2) ≥19.0 U in at least one of the CD samples. Thirty-one genes were finally identified to be "PDC-specific" (Table 3). Through this approach, we tried to extract genes whose expression levels were negligible in all normal pancreatic specimens, but significantly high in at least a part of the cancerous ones. They may be good candidates for molecular markers to develop PCR-based diagnostic tests for PDC.

These potential PDC-specific markers include the genes for FYN protein tyrosine kinase (*FYN*; GenBank accession no. M14676/M14333); insulin-like growth factor binding protein 1 (*IGFBP1*; Y00856); collagen, type I, alpha 1 (*COL1A1*; Z74615); calpain, large polypeptide L2 (*CAPN2*; M23254); eukaryotic translation elongation factor 1 beta 2 (*EEF1B2*; X60489); *AC133* (AF027208) and *CEACAM7* (X98311).

Table 3. Expression level of the PDC-specific genes

Gene symbol	GenBank #	NT	CT #1	CT #2	ND #1	ND #2	ND #3	CD #1	CD #2	CD #3	CD #4	CD #5	CD #6
FYN	M14676	−0.317	−0.982	−0.671	2.198	−1.203	−0.470	3.000	1.327	−0.029	1.435	27.266	13.246
FYN	M14333	−0.642	−0.874	−1.010	1.131	−1.229	0.721	2.771	1.340	−0.032	1.796	28.936	12.357
RGR	U14910	0.174	−1.073	−0.249	−0.795	−0.439	2.719	6.824	1.531	2.929	2.021	1.863	27.514
IGFBP1	Y00856	−0.504	−0.880	−0.671	−0.486	−1.098	−0.461	−1.244	77.812	−0.820	−0.772	52.414	8.442
DUSP1	X68277	0.062	1.488	0.701	1.412	−0.682	1.444	0.782	15.259	0.723	2.374	21.301	2.082
IL1RN	X52015	−0.288	−0.879	−0.489	2.410	−0.874	3.110	−1.102	75.070	1.968	4.507	10.914	5.436
HSJ2	L08069	−0.882	−1.352	−0.752	0.909	−1.269	2.420	−0.992	−0.165	−0.712	0.438	27.059	2.441
APCS	X04608	−0.740	−0.471	−0.212	1.062	−1.140	0.038	−1.127	22.176	6.088	19.942	0.012	−0.482
GTF2A1	U21242	−0.181	−0.754	−0.090	2.395	−1.085	2.376	−0.930	12.423	1.016	−0.140	28.966	7.717
GTF2F2	X16901	−0.697	−1.348	−0.356	−0.392	−0.231	0.523	2.121	3.955	0.329	0.655	20.209	3.319
IRF4	U52682	0.269	−1.213	−0.509	−0.835	0.141	−0.073	−0.561	0.202	−0.103	−0.236	25.817	0.570
POU2AF1	Z49194	−0.698	−1.264	−0.461	−1.069	−0.643	0.090	−0.642	2.758	−0.109	−0.623	47.368	1.189
SNRPG	X85373	−0.374	−1.027	−0.827	2.082	−1.095	3.342	−0.053	11.652	−0.214	−0.355	33.614	7.384
SLC16A3	U81800	0.463	−0.588	0.296	0.712	−0.913	0.332	−0.841	4.999	0.359	−0.222	21.756	0.495
H1F5	X83509	−0.092	−0.239	0.118	1.197	−1.118	0.418	−0.886	1.573	0.166	−0.593	23.560	0.481
GTF2B	M76766	−0.893	−0.670	−0.816	0.824	−1.126	0.467	−1.093	32.156	0.339	4.622	34.587	23.964
SNRPC	M18465	−0.149	−1.184	−0.542	−0.835	−0.403	0.547	−0.610	11.491	0.819	1.282	22.521	1.158
ECM1	U68186	−1.969	−0.882	−0.971	0.048	−0.921	−0.454	−1.218	15.501	0.389	−0.425	50.772	0.072
KLK6	AF013988	−4.069	−1.028	−3.372	−0.121	−1.441	−0.372	−1.324	26.647	0.122	−0.715	60.203	3.603
COL1A1	Z74615	−2.193	0.018	98.459	1.133	−1.197	−0.466	−1.134	10.098	13.086	3.584	131.260	10.451
CAPN2	M23254	−0.996	−1.063	0.483	1.178	−1.387	−0.030	−1.320	12.394	6.932	−0.419	20.623	0.570
RGS5	AB008109	0.026	−0.950	−0.386	−0.837	−1.315	−0.458	−1.093	0.814	0.140	−0.675	0.000	52.133
EEF1B2	X60489	−0.287	−0.713	0.037	1.154	−1.509	2.050	−1.269	9.485	20.314	−0.133	30.121	0.971
F7	M13232	−1.686	−1.055	−0.909	−0.500	−1.476	−0.512	−1.363	−0.254	−0.331	−0.770	−0.353	22.485
CEACAM7	X98311	−0.065	−0.802	−0.728	−0.247	−1.036	−0.085	−0.900	10.468	22.096	0.021	−0.244	−0.011
CAMLG	U18242	−0.703	−0.916	0.285	0.582	−1.435	0.092	−1.238	1.829	1.801	−0.431	22.154	0.461
APOA4	X13629	−3.473	−1.048	−0.974	0.105	−0.835	−0.514	−1.278	−0.240	−0.357	−0.704	−0.324	37.780
GAPDH	M33197	0.142	−0.765	1.590	2.756	−0.920	2.505	−0.854	3.372	3.908	2.241	4.070	21.745
MYBPC3	X84075	−1.825	−1.043	−1.217	−0.475	−1.472	−0.496	−1.283	−0.102	−0.307	−0.772	−0.355	521.712
AC133	AF027208	−0.741	−0.970	−0.666	0.071	−1.527	−0.264	−1.398	19.820	8.152	−0.460	0.546	−0.364
APOBEC1	L25877	−0.740	1.771	−1.215	2.591	1.060	0.982	0.979	9.583	2.584	2.151	12.211	24.971
EIF3S6	U62962	−0.703	0.244	−0.123	2.402	0.053	2.350	−0.626	11.403	28.308	0.607	11.966	6.648

Expression intensities of the "PDC-specific" genes are shown in arbitrary units (U). Gene symbol as well as GenBank accession number (#) is indicated for each gene. Two distinct oligonucleotides were spotted on the array for the *FYN* gene.

Quantitation of mRNA for potential PDC marker genes. Finally, we confirmed the expression of three of the potential PDC marker genes by real-time PCR. Unamplified cDNA was prepared from MUC1$^+$ ductal cells obtained from 8 normal individuals and 10 patients with PDC and was subjected to PCR with primers specific for *β-actin*, *SUMO1*, *AC133*, or *CEACAM7* genes. The amount of each PCR product was monitored in real time, thereby allowing determination of the corresponding C_T values. The abundance of SUMO1, AC133 and CEACAM7 mRNAs was then calculated relative to that of β-actin mRNA.

Consistent with the microarray data, expression of *SUMO1*, *AC133* and *CEACAM7* genes was highly specific to PDC; in particular, the latter two genes were almost silent in normal ductal cells (Fig. 3). These genes are thus candidates for PDC-specific markers. The expression levels of the *SUMO1*, *AC133* and *CEACAM7* genes varied among the cancer specimens, as might be expected from nonuniformity of the transformation process in pancreatic ductal cells.

Discussion

We have demonstrated that a simple comparison of transcriptomes between normal and cancerous tissue of the pancreas is not a suitable approach for characterization of the transformation process. In contrast, through screening with isolated ductal cells derived from normal and carcinoma tissue, we were able to identify a group of genes that may prove helpful in the diagnosis of PDC.

In addition to the purification of PDC cells from pancreatic juice, there is another way to isolate PDC cells, i.e., the laser capture microdissection (LCM) method.[20] Although, with LCM, it is theoretically possible to purify any cell type in a given tissue, fixation and staining procedures of the specimens prior to LCM may severely impair the quality of mRNA in the samples. Furthermore, it would be a demanding task to pick up 10^5–10^6 cells by LCM. Small number of cells obtained by LCM often requires multiple rounds of mRNA amplification before microarray experiments, making the data evaluation more difficult. Therefore, purification of intact and live PDC cells through pancreatic juice would be advantageous for obtaining high-quality mRNA and good reproducibility in transcriptome analysis.

Moreover, as with our CD cases (see Table 1), it is rare to find patients with PDC at early stages competent for surgical resection. Therefore, it may be difficult to complete a large-scale clinical screening of PDC tissue sections. In contrast, screening of hundreds of "pancreatic juice" samples is a realistic project.

For the improvement of PDC treatment, it is essential to detect PDC at the stage of curable carcinoma *in situ*. We assume that the direct analysis of PDC cell-containing specimens would be the most sensitive way to detect PDC, and, in a routine clinical setting, pancreatic juice is the only source to obtain PDC cells. These are the reasons why we attempted to develop a novel PDC diagnosis procedure based on pancreatic juice.

As expected, pancreatic juice contained various amounts of non-ductal cells (mainly blood cells). Therefore, we had first to enrich pancreatic ductal cells from the juice by means of an affinity column directed toward MUC1. It was interesting to find *MUC1* in the "disease-dependent" gene list (Fig. 2C and Table 2). In our analysis, *MUC1* expression was induced in cancerous ductal cells (1.35 U±0.547; mean value±SD) compared to normal ductal cells (0.390 U±0.354). An increase in mRNA[21] or protein[22] level of MUC1 in PDC cells has been also reported. Low yet significant expression of MUC1 in our ductal cell specimens also argues that the MUC1-column eluents did contain pancreatic ductal cells, since MUC1 is expressed only by epithelial cells, not by blood cells.

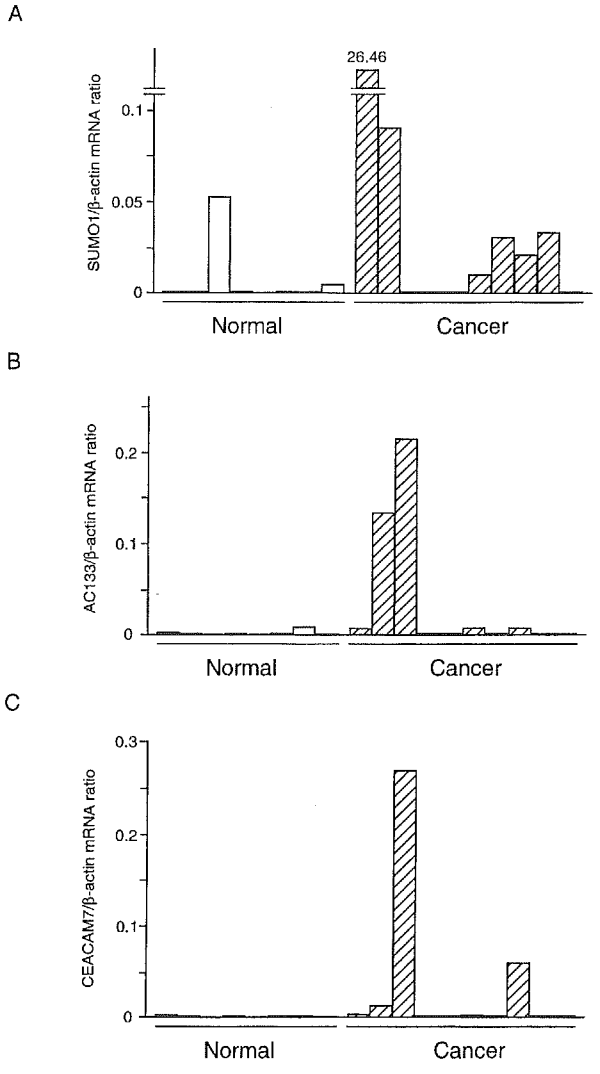

Fig. 3. Quantitation of *SUMO1*, *AC133* and *CEACAM7* gene transcripts in MUC1$^+$ ductal cells. Complementary DNA prepared from pancreatic ductal cells of 8 normal individuals and 10 PDC patients was subjected to real-time PCR with primers specific for *SUMO1* (A), *AC133* (B), *CEACAM7* (C), or *β-actin* genes. The ratio of the abundance of the target transcripts to that of β-actin mRNA was calculated as 2^n, where n is the C_T value for β-actin cDNA minus the C_T value of the target cDNA.

Our MUC1-based purification system does not discriminate normal ductal cells from malignant ones. Therefore, ductal cells isolated from PDC patients (such as CD #1–6) should be a mixture of normal ductal cells and PDC ones. Since there are no cell membrane proteins known to be specifically expressed in PDC, it is currently impossible to directly purify PDC cells from pancreatic juice. Rather, we here aimed to develop a sensitive method to detect a trace amounts of PDC cells shed into pancreatic juice.

For this purpose, there may be two distinct types of molecular markers. One type is useful in statistically distinguishing normal and cancerous ductal cell types. Such analyses choose genes whose expression level has a small deviation, and, therefore, may be suitable to construct custom-made DNA microarrays. Genes of the other type would be active only in cancerous ductal cells, but strictly absent in normal ones. These genes would be good candidates for the target transcripts used in RT-PCR-based detection systems. Expression levels of such genes in cancerous cells may have a relatively large SD, and such genes may not be expressed in all cancerous cells. However, if

their transcription is completely silent in normal cells, an RT-PCR-based detection kit would be of practical value. The genes in Tables 2 and 3 are our first results from the approaches above, and expression profiles of some of them were confirmed by real-time PCR (Fig. 3).

Among the genes listed in Tables 2 and 3, several were already known to be highly expressed in carcinoma cells. For example, ID2 drives cell cycle progression by interacting with, and suppressing the activity of, a tumor suppressor, Rb.[23] ID2 can also suppress another growth suppressor, p16.

CEACAM7 belongs to the CEA family of proteins. In contrast to the high level of expression of CEA apparent in colorectal carcinomas, CEACAM7 is abundant in normal colonic epithelium and its expression is down-regulated during malignant transformation.[24, 25] Although its expression in pancreas has not been well characterized, previous data indicate that CEACAM7 is expressed in normal pancreatic ductal cells.[24] However, our observation that the *CEACAM7* gene is preferentially expressed in ductal cells of PDC patients suggests that this gene is a potential marker for cancer diagnosis with either ductal cell- or serum-based assays.

AC133 was initially identified as a cell surface marker specific to a hematopoietic stem cell-enriched fraction with a $CD34^{high}$, $CD38^{low}$ or $CD38^{-}$, and c-Kit^{+} phenotype.[26] This protein is also expressed on the precursor of endothelial cells,[27] indicating that it may be a marker for immature hemangioblasts, which are common precursors for blood cells and blood vessels. Although expression of AC133 in tissues other than bone marrow and the retina has not been previously demonstrated, we have now shown that the *AC133* gene is expressed in the pancreatic ductal cells of PDC patients. Given the abundance of AC133 in normal hemangioblasts, the expression of the *AC133* gene in carcinoma ductal cells may suggest that AC133 is also a marker of the precursor for ductal cells. The increased expression of the *AC133* gene in PDC may thus reflect the immature nature of the cancer cells with regard to the differentiation program of ductal cells.

It should be noted, however, that none of the single genes listed in Tables 2 and 3 was able to distinguish all PDC samples from normal ductal cells. In addition to such single gene-based prediction systems, it may be possible to use the expression profiles of a combination of "class predictor" genes[28] for PDC diagnosis. We have indeed examined the feasibility of this approach with the statistically "disease-dependent" genes listed in Table 2. Prediction of PDC diagnosis was tried with the k-nearest neighbor algorithm by using the GeneSpring software (http://www.silicongenetics.com/Support/GeneSpring/GSnotes/class_prediction.pdf). In a "cross-validation" trial, all three ND samples were correctly diagnosed by the expression profiles of the disease-dependent genes (data not shown). With regard to the CD samples, four out of six samples were correctly predicted, and the other two were called "unpredictable." Therefore, among the nine ductal cell specimens, seven (77.8%) were correctly diagnosed. Selection of stronger "predictor" genes through large-scale microarray studies may make it possible to construct reliable "PDC diagnosis arrays" harboring a small number of such predictor genes.

In conclusion, we have shown that DNA microarray analysis with purified ductal cell fractions is a promising approach to the identification of PDC-specific genes, being greatly superior to a mere comparison of tissue specimens. Our data thus provide a basis for the possible development of an ERCP-dependent sensitive and specific test for the detection of pancreatic cancer.

This work was supported in part by a Grant-in-Aid for Scientific Research (C) from the Ministry of Education, Culture, Sports, Science and Technology, Japan.

1. Bornman PC, Beckingham IJ. Pancreatic tumours. *Br Med J* 2001; **322**: 721–3.
2. Rosewicz S, Wiedenmann B. Pancreatic carcinoma. *Lancet* 1997; **349**: 485–9.
3. Adamek HE, Albert J, Breer H, Weitz M, Schilling D, Riemann JF. Pancreatic cancer detection with magnetic resonance cholangiopancreatography and endoscopic retrograde cholangiopancreatography: a prospective controlled study. *Lancet* 2000; **356**: 190–3.
4. Kondo H, Sugano K, Fukayama N, Kyogoku A, Nose H, Shimada K, Ohkura H, Ohtsu A, Yoshida S, Shimosato Y. Detection of point mutations in the K-ras oncogene at codon 12 in pure pancreatic juice for diagnosis of pancreatic carcinoma. *Cancer* 1994; **73**: 1589–94.
5. Sugano K, Nakashima Y, Yamaguchi K, Fukayama N, Maekawa M, Ohkura H, Kakizoe T, Sekiya T. Sensitive detection of loss of heterozygosity in the TP53 gene in pancreatic adenocarcinoma by fluorescence-based single-strand conformation polymorphism analysis using blunt-end DNA fragments. *Genes Chromosom Cancer* 1996; **15**: 157–64.
6. Caldas C, Hahn SA, da Costa LT, Redston MS, Schutte M, Seymour AB, Weinstein CL, Hruban RH, Yeo CJ, Kern SE. Frequent somatic mutations and homozygous deletions of the p16 (MTS1) gene in pancreatic adenocarcinoma. *Nat Genet* 1994; **8**: 27–32.
7. Hahn SA, Schutte M, Hoque AT, Moskaluk CA, da Costa LT, Rozenblum E, Weinstein CL, Fischer A, Yeo CJ, Hruban RH, Kern SE. DPC4, a candidate tumor suppressor gene at human chromosome 18q21.1. *Science* 1996; **271**: 350–3.
8. Hohne MW, Halatsch ME, Kahl GF, Weinel RJ. Frequent loss of expression of the potential tumor suppressor gene DCC in ductal pancreatic adenocarcinoma. *Cancer Res* 1992; **52**: 2616–9.
9. Furuya N, Kawa S, Akamatsu T, Furihata K. Long-term follow-up of patients with chronic pancreatitis and K-ras gene mutation detected in pancreatic juice. *Gastroenterology* 1997; **113**: 593–8.
10. Duggan DJ, Bittner M, Chen Y, Meltzer P, Trent JM. Expression profiling using cDNA microarrays. *Nat Genet* 1999; **21**: 10–4.
11. Schena M, Shalon D, Davis RW, Brown PO. Quantitative monitoring of gene expression patterns with a complementary DNA microarray. *Science* 1995; **270**: 467–70.
12. Miyazato A, Ueno S, Ohmine K, Ueda M, Yoshida K, Yamashita Y, Kaneko T, Mori M, Kirito K, Toshima M, Nakamura Y, Saito K, Kano Y, Furusawa S, Ozawa K, Mano H. Identification of myelodysplastic syndrome-specific genes by DNA microarray analysis with purified hematopoietic stem cell fraction. *Blood* 2001; **98**: 422–7.
13. Van Gelder RN, von Zastrow ME, Yool A, Dement WC, Barchas JD, Eberwine JH. Amplified RNA synthesized from limited quantities of heterogeneous cDNA. *Proc Natl Acad Sci USA* 1990; **87**: 1663–7.
14. Balague C, Audie JP, Porchet N, Real FX. *In situ* hybridization shows distinct patterns of mucin gene expression in normal, benign, and malignant pancreas tissues. *Gastroenterology* 1995; **109**: 953–64.
15. Terada T, Ohta T, Sasaki M, Nakamura Y, Kim YS. Expression of MUC apomucins in normal pancreas and pancreatic tumours. *J Pathol* 1996; **180**: 160–5.
16. Lacobuzio-Donahue CA, Maitra A, Shen-Ong GL, van Heek T, Ashfaq R, Meyer R, Walter K, Berg K, Hooingsworth MA, Cameron JL, Yeo CJ, Kern SE, Goggins M, Hruban RH. Discovery of novel tumor markers of pancreatic cancer using global gene expression technology. *Am J Pathol* 2002; **160**: 1239–49.
17. Alon U, Barkai N, Notterman DA, Gish K, Ybarra S, Mack D, Levine AJ. Broad patterns of gene expression revealed by clustering analysis of tumor and normal colon tissues probed by oligonucleotide arrays. *Proc Natl Acad Sci USA* 1999; **96**: 6745–50.
18. Hay RT. Protein modification by SUMO. *Trends Biochem Sci* 2001; **26**: 332–3.
19. Johnson ES, Gupta AA. An E3-like factor that promotes SUMO conjugation to the yeast septins. *Cell* 2001; **106**: 735–44.
20. Luo L, Salunga RC, Guo H, Bittner A, Joy KC, Galindo JE, Xiao H, Rogers KE, Wan JS, Jackson MR, Erlander MG. Gene expression profiles of laser-captured adjacent neuronal subtypes. *Nat Med* 1999; **5**: 117–22.
21. Ho SB, Niehans GA, Lyftogt C, Yan PS, Cherwitz DL, Gum ET, Dahiya R, Kim YS. Heterogeneity of mucin gene expression in normal and neoplastic tissues. *Cancer Res* 1993; **53**: 641–51.
22. Osako M, Yonezawa S, Siddiki B, Huang J, Ho JJL, Kim YS, Sato E. Immunohistochemical study of mucin carbohydrates and core proteins in human pancreatic tumors. *Cancer* 1993; **71**: 2191–9.
23. Lavarone A, Garg P, Lasorella A, Hsu J, Israel MA. The helix-loop-helix protein Id-2 enhances cell proliferation and binds to the retinoblastoma protein. *Genes Dev* 1994; **8**: 1270–84.
24. Scholzel S, Zimmermann W, Schwarzkopf G, Grunert F, Rogaczewski B, Thompson J. Carcinoembryonic antigen family members CEACAM6 and

CEACAM7 are differentially expressed in normal tissues and oppositely deregulated in hyperplastic colorectal polyps and early adenomas. *Am J Pathol* 2000; **156**: 595–605.
25. Thompson J, Seitz M, Chastre E, Ditter M, Aldrian C, Gespach C, Zimmermann W. Down-regulation of carcinoembryonic antigen family member 2 expression is an early event in colorectal tumorigenesis. *Cancer Res* 1997; **57**: 1776–84.
26. Hin AH, Miraglia S, Zanjani ED, Almeida-Porada G, Ogawa M, Leary AG, Olweus J, Kearney J, Buck DW. AC133, a novel marker for human hematopoietic stem and progenitor cells. *Blood* 1997; **90**: 5002–12.
27. Gallacher L, Murdoch B, Wu DM, Karanu FN, Keeney M, Bhatia M. Isolation and characterization of human CD34(−)Lin(−) and CD34(+)Lin(−) hematopoietic stem cells using cell surface markers AC133 and CD7. *Blood* 2000; **95**: 2813–20.
28. Golub TR, Slonim DK, Tamayo P, Huard C, Gaasenbeek M, Mesirov JP, Coller H, Loh ML, Downing JR, Caligiuri MA, Bloomfield CD, Lander ES. Molecular classification of cancer: class discovery and class prediction by gene expression monitoring. *Science* 1999; **286**: 531–7.

Leukemia (2003) 17, 1990–1997

www.nature.com/leu

DNA microarray analysis of hematopoietic stem cell-like fractions from individuals with the M2 subtype of acute myeloid leukemia

Y Oshima[1], M Ueda[2], Y Yamashita[3], YL Choi[3], J Ota[3], S Ueno[3,4], R Ohki[3,4], K Koinuma[3,5], T Wada[3,6], K Ozawa[2], A Fujimura[1] and H Mano[3,7]

[1]*Division of Clinical Pharmacology, Jichi Medical School, Yakushiji, Kawachigun, Tochigi, Japan;* [2]*Division of Hematology, Jichi Medical School, Yakushiji, Kawachigun, Tochigi, Japan;* [3]*Division of Functional Genomics, Jichi Medical School, Yakushiji, Kawachigun, Tochigi, Japan;* [4]*Division of Cardiology, Jichi Medical School, Yakushiji, Kawachigun, Tochigi, Japan;* [5]*Department of Surgery, Jichi Medical School, Yakushiji, Kawachigun, Tochigi, Japan;* [6]*Department of Gynecology, Jichi Medical School, Yakushiji, Kawachigun, Tochigi, Japan; and* [7]*CREST, JST, Saitama, Japan*

Acute myeloid leukemia (AML) may develop *de novo* or secondarily to myelodysplastic syndrome (MDS). Although the clinical outcome of MDS-related AML is worse than that of *de novo* AML, it is not easy to differentiate between these two clinical courses without a record of prior MDS. Large-scale profiling of gene expression by DNA microarray analysis is a promising approach with which to identify molecular markers specific to *de novo* or MDS-related AML. This approach has now been adopted with AC133-positive hematopoietic stem cell-like fractions purified from 10 individuals, each with either *de novo* or MDS-related AML of the M2 subtype. Sets of genes whose activity was associated with either disease course were identified. Furthermore, on the basis of the expression profiles of these genes, it was possible to predict correctly the clinical diagnosis for 17 (85%) of the 20 cases in a cross-validation trial. Similarly, different sets of genes were identified whose expression level was associated with clinical outcome after induction chemotherapy. These data suggest that, at least in terms of gene expression profiles, *de novo* AML and MDS-related AML are distinct clinical entities.
Leukemia (2003) **17**, 1990–1997. doi:10.1038/sj.leu.2403098
Keywords: DNA microarray; acute myeloid leukemia; myelodysplastic syndrome; *DLK*, M2 subtype

Introduction

Myelodysplastic syndrome (MDS) is a clonal disorder of hematopoietic stem cells (HSCs) that affects mostly the elderly (median age of 70 years). MDS is characterized by two clinical manifestations: (i) cytopenia in peripheral blood despite hyper- or normal cellularity in bone marrow (BM), a condition referred to as ineffective hematopoiesis, and (ii) dysplastic changes in blood cells.[1] It is a multistage syndrome, the early stages of which are termed refractory anemia (RA), RA with ringed sideroblasts, or refractory cytopenia with multilineage dysplasia (RCMD).[2]

Between 10 and 50% of cases of MDS, especially those associated with unfavorable chromosomal abnormalities, eventually undergo malignant transformation into MDS-related acute myeloid leukemia (AML), the outcome of which is poor.[3,4] The blasts of individuals with MDS are, in general, refractory to chemotherapeutic agents, and a cure for this condition is rarely achievable except in cases in which allogeneic BM transplantation is applicable. It is therefore clinically important to be able to differentiate between individuals with *de novo* AML and those with MDS-related AML.

Correspondence: Dr H Mano, Division of Functional Genomics, Jichi Medical School, 3311-1 Yakushiji, Kawachigun, Tochigi 329-0498, Japan; Fax: +81 285 44 7322
Received 9 April 2003; accepted 19 June 2003

However, such differentiation is not always an easy task. Some types of dysplasia are apparent even in BM cells of healthy people and such changes become more prominent in the elderly.[5,6] Chromosomal anomalies often associated with MDS, including those affecting chromosomes 5 and 7, are also manifest in some *de novo* AML blasts and indeed are an indicator of poor prognosis in AML patients. It is therefore often difficult to diagnose correctly elderly individuals with AML and dysplastic changes if knowledge of a preceding history of MDS is not available.

Complicating issues even further, certain cases of *de novo* AML (with the absence of prior MDS history or anticancer treatment) may be associated with prominent blood cell dysplasia. The recent proposal for AML classification by the World Health Organization stipulates that individuals with AML and dysplastic cells be diagnosed with AML with multilineage dysplasia (AML-MLD), irrespective of whether the AML is *de novo* or secondary to MDS.[7] It remains to be determined whether AML-MLD is an amalgamation of clinical entities with distinct mechanisms as well as prognoses.

DNA microarray analysis allows the monitoring of the levels of expression of thousands of genes simultaneously[8] and may therefore help to identify molecular markers that differentiate *de novo* AML from MDS-related AML. However, a simple comparison of BM mononuclear cells (MNCs) between these two conditions may be problematic. The cell composition of BM MNCs differs markedly among individuals. Differences in the gene expression profiles between BM MNCs from a given pair of individuals may thus reflect these differences in cell composition. The elimination of such pseudopositive and pseudonegative data necessitates the purification of background-matched cell fractions from the clinical specimens before microarray analysis.

Given that MDS results from a transformation of HSC clones, HSCs are an appropriate target for purification and gene expression analysis. With the use of an affinity purification procedure based on the HSC-specific surface protein AC133,[9] we have therefore initiated a nationwide project aimed at the purification and storage of HSC-like fractions from individuals with leukemia and related disorders in Japan. To date, more than 400 purified cell fractions have been deposited in this 'Blast Bank.'

To further reduce the influence of differentiation commitment of blasts toward certain lineages, we selected for the present study only those Blast Bank samples with the same phenotype, the M2 subtype according to the classification of the French–American–British (FAB) Cooperative Group.[10] We thus characterized the expression profiles of >12 000 genes in $AC133^+$ Blast Bank samples from 10 patients with *de novo* AML of the M2 subtype as well as from 10 individuals with MDS-related

AML of the M2 subtype. Comparison of the microarray data revealed gene markers of potential clinical utility for the diagnosis and prediction of response to chemotherapy.

Materials and methods

Purification of AC133$^+$ cells

BM aspirates were obtained from subjects with written informed consent and the AC133$^+$ HSC-like fraction was purified from each specimen as described previously.[11,12] In brief, MNCs were isolated by Ficoll–Hypaque density gradient centrifugation, labeled with AC133 MicroBeads (Miltenyi Biotec, Auburn, CA, USA), and subjected to chromatography on a mini-MACS magnetic cell separation column (Miltenyi Biotec). Enrichment of the HSC-like fraction was evaluated by subjecting portions of the MNC and AC133$^+$ cell preparations either to staining with Wright–Giemsa solution or to analysis of the expression of CD34, CD38, and AC133 by flow cytometry (FACScan; Becton Dickinson, Mountain View, CA, USA). In most instances, the CD34^{high}CD38^{low} fraction constituted >90% of the eluate of the affinity column.

DNA microarray analysis

Total RNA was extracted from the AC133$^+$ cell preparations by the acid guanidinium method and was subjected to two rounds of amplification with T7 RNA polymerase as described.[13] A total of 1 μg of the amplified cRNA was then converted to double-stranded cDNA, which was used to prepare biotin-labeled cRNA for hybridization with GeneChip HGU95Av2 microarrays (Affymetrix, Santa Clara, CA, USA) harboring oligonucleotides corresponding to a total of 12 625 genes. Hybridization, washing, and detection of signals on the arrays were performed with the GeneChip system (Affymetrix). To evaluate the fidelity of the RNA amplification procedure, we subjected total RNA and cRNA after one (aRNA1) or two (aRNA2) rounds of amplification from the same patient sample independently to the hybridization with the GeneChip system. The resulting expression intensities yielded Pearson's correlation coefficients of 0.807 for total RNA and aRNA1 and of 0.931 for aRNA1 and aRNA2. In the same experiments, the ratio of the number for genes with 'Present' call and those with 'Absent' call was calculated to be 0.261 for total RNA, 0.303 for aRNA1, and 0.171 for aRNA2.

Statistical analysis

The fluorescence intensity for each gene was normalized relative to the fluorescence value for the 50th percentile gene with a 'Present' or 'Marginal' call (Microarray Suite 4.0, Affymetrix) in each hybridization. Hierarchical clustering of the data set and isolation of diagnosis-related genes were performed with GeneSpring 5.0.3 software (Silicon Genetics, Redwood, CA, USA). All raw array data as well as details of the genes shown in the figures are available as supplementary information at the *Leukemia* web site. The raw array data will also be accessible from the Array-Express web site (http://www.ebi.ac.uk/arrayexpress).

Real-time reverse transcription-polymerase chain reaction (RT-PCR) analysis

Portions of nonamplified cDNA were subjected to PCR with a QuantiTect SYBR Green PCR Kit (Qiagen, Valencia, CA, USA). The amplification protocol comprised incubations at 94°C for 15 s, 60°C for 30 s, and 72°C for 60 s. The annealing temperature was raised up to 63°C only for the amplification of the topoisomerase IIβ (TOPIIB) cDNA. Incorporation of the SYBR Green dye into PCR products was monitored in real time with an ABI PRISM 7700 sequence detection system (PE Applied Biosystems, Foster City, CA, USA), thereby allowing determination of the threshold cycle (C_T) at which exponential amplification of PCR products begins. The C_T values for cDNAs corresponding to the glyceraldehyde-3-phosphate dehydrogenase (GAPDH), *DLK* and *TOPIIB* genes were used to calculate the abundance of *DLK* or *TOPIIB* mRNA relative to that of *GAPDH* mRNA. The oligonucleotide primers for PCR were 5′-GTCAGTGGTGGACCTGACCT-3′ and 5′-TGAGCTTGACAA AGTGGTCG-3′ for *GAPDH* cDNA; 5′-ATCCTGAAGGTGTC CATGAAAG-3′ and 5′-GCACTTGTTGAGGAAGACGATAC-3′ for *DLK* cDNA; and 5′-AGTTGGAAGAGACAATGCCCTC AC-3′ and 5′-TACCAGGCTCCTTCTTCTCCCTCT-3′ for *TOPIIB* cDNA.

Results

Purification of Blast Bank cells

To demonstrate the utility of the Blast Bank strategy, we previously compared the expression of the CD34 gene between BM MNCs and AC133$^+$ cells by microarray analysis.[11] The expression level of the gene was 519 and 42 322 arbitrary units (U) in a healthy volunteer and a patient with MDS-related AML, respectively, in the analysis of BM MNCs. However, in the analysis of AC133$^+$ cells from the same two individuals, the expression levels were 6 749 546 and 5 543 512 U in the volunteer and patient, respectively. The apparent induction of the CD34 gene in the MNCs of the patient thus actually reflected the expansion of the immature blasts expressing this gene.

From our Blast Bank depository, we selected 20 specimens derived from individuals with AML of the FAB M2 subtype, half of them ($n=10$) with *de novo* AML and the other half ($n=10$) with MDS-related AML. The clinical characteristics of the 20 patients are summarized in Table 1. The M2-specific karyotype anomaly, t(8;21), was apparent in five of the *de novo* AML patients, but in none of those with MDS-related AML. All patients were treated with anthracyclin- and/or cytarabine-based regimens, with most of those with MDS-related AML being refractory to treatment.

For the expression profiling of AC133$^+$ cells to be meaningful, such fractions should contain substantial numbers of leukemic clones. We were able to purify $>1\times10^6$ AC133$^+$ cells from the BM MNCs of our patients with AML M2, whereas the yield of AC133$^+$ cells was only 1000–5000 cells from similar starting numbers of BM MNCs obtained from healthy volunteers (data not shown). The purified HSC-like fractions from individuals with AML thus likely consist predominantly of leukemic HSC-like cells. This conclusion was supported by our observation that, for one individual with MDS-related leukemia, fluorescence *in situ* hybridization analysis revealed a −5q anomaly in only 54% of BM MNCs but in 96% of the corresponding purified AC133$^+$ cells (data not shown).

Table 1 Clinical characteristics of the patients subjected to microarray analysis

Patient	*Disease*	*Response*	*Karyotype*
AML-1	AML	Failure	−7
AML-2	AML	Failure	−7
AML-3	AML	CR	−7
AML-4	AML	CR	t(8;21)
AML-5	AML	CR	t(8;21)
AML-6	AML	Failure	Normal
AML-7	AML	CR	Normal
AML-8	AML	CR	t(8;21)
AML-9	AML	CR	t(8;21)
AML-10	AML	CR	t(8;21)
MDS-1	MDS	Failure	+8
MDS-2	MDS	Failure	+8
MDS-3	MDS	Failure	Other
MDS-4	MDS	Failure	Normal
MDS-5	MDS	Failure	+8
MDS-6	MDS	Failure	+8
MDS-7	MDS	CR	Other
MDS-8	MDS	Failure	Normal
MDS-9	MDS	Failure	Normal
MDS-10	MDS	Failure	+8

AML, *de novo* AML; MDS, MDS-related AML. The Response column indicates the clinical outcome of the first induction chemotherapy; CR, complete remission.

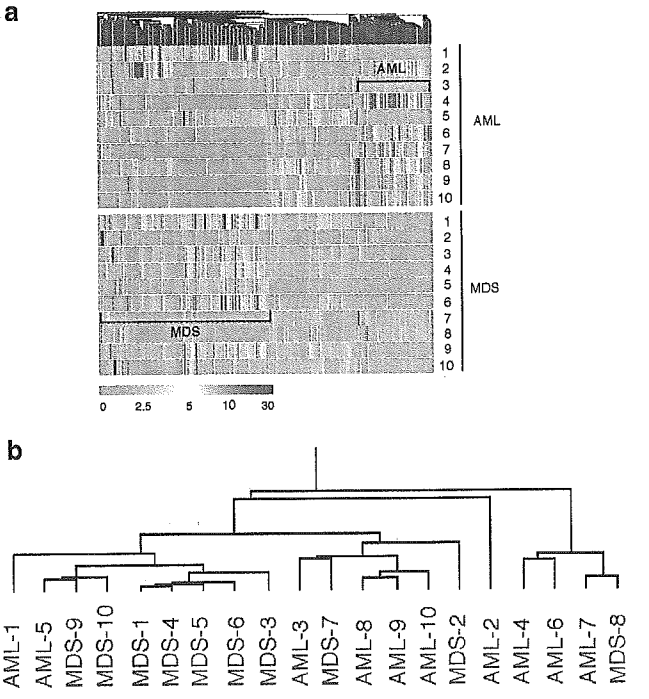

Figure 1 Expression profiles of 6672 genes in leukemic blasts. (a) Hierarchical clustering of 6672 genes on the basis of their expression profiles in Blast Bank samples derived from 10 individuals, each with either *de novo* AML (AML) or MDS-related AML (MDS). Each column represents a single gene on the microarray, and each row a separate patient sample. The positions of large clusters of genes that were expressed preferentially in blasts from patients with *de novo* AML or in those from the patients with MDS-related AML are indicated in blue. (b) Two-way clustering analysis of the *de novo* AML (blue) and MDS-related AML (red) patients based on the similarities in the expression profiles of the 6672 genes shown in (a).

Transcriptome of AML M2 blasts

From the expression data obtained for the >12 000 human genes in the 20 samples analyzed, we first selected genes whose expression received the 'Present' call from the Microarray Suite 4.0 software in at least 10% of the samples, in order to exclude genes that were virtually silent transcriptionally. A total of 6672 genes passed this 'selection window', and their expression profiles in the 20 samples are shown in Figure 1a as a dendrogram, or 'gene tree', in which genes with similar expression profiles (assessed by standard correlation) among the samples are clustered near each other. Clusters of genes that were expressed preferentially in either the *de novo* AML blasts or the MDS-related AML blasts were thus revealed. The genes preferentially expressed in the MDS-related AML blasts were expressed at a substantial level in the blasts from only one (AML-1) of the patients with *de novo* AML.

To evaluate statistically the similarity of the overall gene expression profiles among the 20 samples, we generated another dendrogram, a 'patient tree,' by the two-way clustering method[14] with a separation ratio of 1.0 (Figure 1b). The samples did not cluster into two major disease-specific branches; rather, *de novo* AML and MDS-related AML cases were mixed in several branches.

Identification of disease-associated genes

To identify genes whose expression might allow differentiation between *de novo* AML and MDS-related AML, we first examined those whose expression level differed significantly between the two groups of samples (Welch ANOVA test, $P<0.01$). A total of 574 such genes were identified. Most of these genes, however, were expressed at a low level in both types of specimens, rendering their utility as diagnostic markers uncertain. From these 574 genes, we therefore selected those whose mean expression intensity differed by ≥5.0 U between the two groups. The resulting 57 'disease-associated' genes are shown in a gene-tree format in Figure 2a; 52 of these genes were specific to MDS-related AML and the remaining five were specific to *de novo* AML. The former group of genes included those for proteins important in regulation of the cell cycle (cyclin D3, GenBank accession number M92287; cyclin I, D50310; CDC10, S72008), in protein synthesis (elongation factor 1α, J04617; eIF4, D30655; elongation factor 1γ-related protein, M55409; elongation factor 2, Z11692; eIF3 p47 subunit, U94855; elongation factor 1α-2, X70940; ribosomal protein S19, M81757; ribosomal protein S4, M58458; ribosomal protein S6, X67309), and in transcriptional regulation (CtBP, U37408; ERF-2, X78992; SP1, X68194). We next performed two-way clustering analysis of the 20 patients based on the expression levels of such 57 disease-associated genes (Figure 2b). The patients clustered into two major branches, one containing only those with *de novo* AML and the other containing mostly those with MDS-related AML.

We also performed 'class prediction' analysis for the samples with GeneSpring software and with the 57 disease-associated genes as the 'class predictor' (http://www.silicongenetics.com/Support/GeneSpring/GSnotes/class_prediction.pdf). In a cross-validation ('drop-one-out') format, the '*k*-nearest-neighbor' samples were counted in Euclidean distance for a 'dropped' sample, and the proportion of neighbor samples from each class was used to calculate the prediction *P*-value for each class (*de novo* AML or MDS-related AML). The resulting class predictions with a *P*-value ratio of <0.2 were determined to be significant. The disease prediction matched the clinical diagnosis for 17

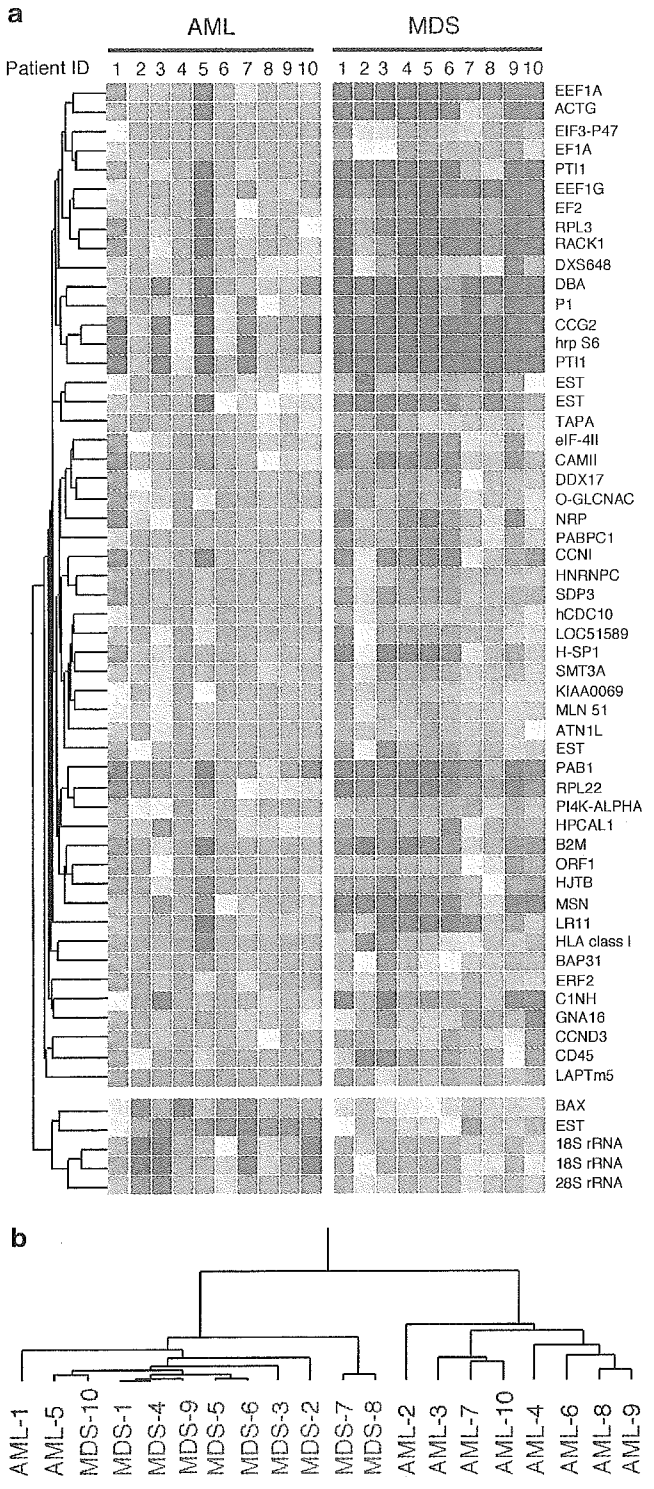

Figure 2 Identification of disease-associated genes. (a) Expression profiles of 57 disease-associated genes in a dendrogram color coded as indicated by the scale in Figure 1a. Each row corresponds to a single gene, and each column to AC133$^+$ cells from a patient with *de novo* AML (AML) or MDS-related AML (MDS). The gene symbols are indicated on the right. The names, accession numbers, and expression intensity data for these genes are available at the Leukemia web site. (b) Two-way clustering analysis of the 20 samples based on the expression levels of the disease-associated genes.

(85%) of the 20 patients; two cases (AML-1 and MDS-8) were not predictable and one case (AML-5) yielded a predicted diagnosis that differed from the clinical one (Table 2).

Table 2 Diagnosis prediction based on gene expression profiles

Patient	*Clinical diagnosis*	*Predicted diagnosis*	*P-value ratio*
AML-1	AML	Unpredictable	0.475
AML-2	AML	AML	0.000
AML-3	AML	AML	0.000
AML-4	AML	AML	0.000
AML-5	AML	MDS	0.000
AML-6	AML	AML	0.000
AML-7	AML	AML	0.000
AML-8	AML	AML	0.000
AML-9	AML	AML	0.000
AML-10	AML	AML	0.000
MDS-1	MDS	MDS	0.000
MDS-2	MDS	MDS	0.019
MDS-3	MDS	MDS	0.000
MDS-4	MDS	MDS	0.000
MDS-5	MDS	MDS	0.019
MDS-6	MDS	MDS	0.000
MDS-7	MDS	MDS	0.13
MDS-8	MDS	Unpredictable	0.255
MDS-9	MDS	MDS	0.000
MDS-10	MDS	MDS	0.000

Prediction of chemosensitivity

Seven of the patients with *de novo* AML and one patient with MDS-related AML (the CR group) underwent complete remission (CR) after the first induction chemotherapy, whereas three patients with *de novo* AML and nine patients with MDS-related AML (the Failure group) did not exhibit a sufficient reduction in the number of immature blasts in their BM in response to such treatment (Table 1). Given that all Blast Bank samples in this study were obtained prior to chemotherapy, we next examined whether it was possible to predict treatment outcome on the basis of the gene expression profiles of the blasts.

For this purpose, we first selected from the 6672 genes expressed in the AC133$^+$ cells of the various patients those whose expression levels differed significantly between the CR and Failure groups (Welch ANOVA, $P<0.01$). The resulting 1353 genes were then examined for those whose mean expression level differed by $\geqslant 5.0$ U between the two groups. A total of 37 'outcome-associated' genes were so identified, 33 of which were preferentially expressed in the Failure group and the remaining four of which were expressed selectively in the CR group (Figure 3a). Unexpectedly, only 16 genes were common to both the disease- and outcome-associated genes.

The genes associated with treatment failure included those for the transcription factor c-FOS (GenBank accession number, V01512), TOPIIB (X68060), INT6 (U62962), and sorting nexin 3 (AF034546). Topoisomerase is a target for anticancer drugs, such as etoposide, that are routinely used in the current treatment of AML.[15] A high level of TOPIIB expression might therefore contribute to drug resistance in the Failure group. To confirm the outcome-dependent expression of *TOPIIB* gene, we examined the mRNA level of *TOPIIB* by the quantitative RT-PCR analysis. As shown in Figure 3b, *TOPIIB* mRNA was abundant only in the leukemic blasts isolated from individuals with drug-resistant AML.

Two-way clustering analysis based on the expression profiles of the 37 outcome-associated genes yielded two major branches: one containing all eight samples in the CR group and two Failure samples, and the other containing the remaining 10 samples in the Failure group (Figure 3c).

We also performed class prediction analysis with the 37 outcome-associated genes as we did with the disease-associated genes. The clinical response of 15 (75%) of the 20 cases was successfully predicted, that of three cases was not predictable, and that of the remaining two cases was predicted incorrectly (Table 3).

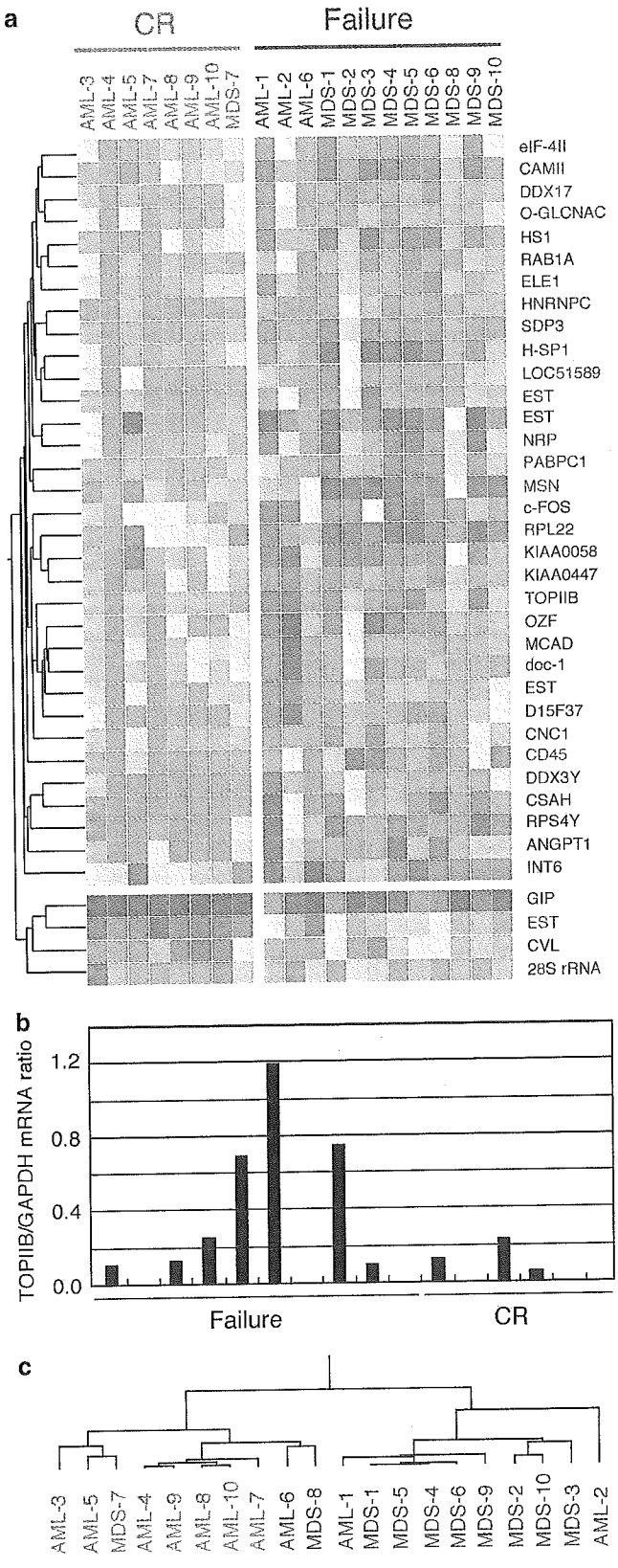

Figure 3 Identification of clinical outcome-associated genes. (a) Expression profiles of 37 outcome-associated genes are shown in a dendrogram color coded as indicated by the scale in Figure 1a. Each row corresponds to a single gene, and each column to AC133$^+$ cells from a patient who underwent CR after induction chemotherapy or in whom treatment failed (Failure). The gene symbols are indicated at the right. The genes also identified in Figure 2a are shown in red. (b) Quantitation of TOPIIB mRNA in AC133$^+$ blasts. Complementary DNA was prepared from the AML M2 blasts of the CR and Failure groups and was subjected to real-time PCR analysis with primers specific for the TOPIIB or GAPDH genes. The ratio of the abundance of TOPIIB mRNA to that of GAPDH mRNA was calculated as 2^{-n}, where n is the C_T value for GAPDH cDNA minus the C_T value for TOPIIB cDNA. (c) Two-way clustering analysis of the 20 samples based on the expression levels of the outcome-associated genes. CR and Failure samples are shown in green and purple, respectively.

Identification of single gene markers for chemosensitivity

The gene sets identified in Figures 2a and 3a may represent candidate genes for the construction of custom-made DNA microarrays for disease diagnosis and prediction of clinical outcome, respectively. Given that the availability of DNA microarray systems is still limited in hospitals, however, it would be beneficial to identify a single gene whose expression (at the mRNA or protein level) could be used as a reliable marker for such purposes. For example, it would be useful to be able to predict the drug sensitivity of leukemic blasts by flow cytometric analysis of a cell surface protein. It is unlikely, however, that determination of the expression of any single gene will allow correct diagnosis or prediction of drug sensitivity for all samples. We therefore attempted to identify individual genes whose high expression level might be sufficient to predict drug resistance, but the absence of which may not necessarily imply drug sensitivity. Such predictor genes would thus be inactive in leukemic blasts from all drug-sensitive patients but be active in samples from at least some proportion of drug-resistant individuals.

Table 3 Prediction of response to chemotherapy

Patient	*Clinical outcome*	*Prediction*	*P-value ratio*
AML-1	Failure	Failure	0.007
AML-2	Failure	Unpredictable	0.366
AML-3	CR	CR	0.029
AML-4	CR	CR	0.029
AML-5	CR	CR	0.187
AML-6	Failure	CR	0.006
AML-7	CR	CR	0.029
AML-8	CR	CR	0.002
AML-9	CR	CR	0.029
AML-10	CR	CR	0.002
MDS-1	Failure	Failure	0.007
MDS-2	Failure	Unpredictable	0.943
MDS-3	Failure	Failure	0.007
MDS-4	Failure	Failure	0.007
MDS-5	Failure	Failure	0.007
MDS-6	Failure	Failure	0.007
MDS-7	CR	CR	0.029
MDS-8	Failure	CR	0.006
MDS-9	Failure	Failure	0.007
MDS-10	Failure	Unpredictable	0.943

We first calculated the mean expression levels of each of the 6672 expressed genes in both the CR and Failure groups. Then, with the use of the GeneSpring software, we searched for genes whose expression profiles were significantly similar, with a minimum correlation of 0.95, to that of a hypothetical 'Failure-specific gene' with a mean expression level of 0.0 U in the CR group and of 100.0 U in the Failure group. From the 2354 such genes identified, we then selected those whose expression value was both <3.0 U in all CR samples and $\geqslant 10.0$ U in at least one of the Failure samples. A total of 42 genes was thus shown to be 'Failure specific' (Figure 4a), of which we examined those with the fewest false-positive results (while allowing false-negative ones). The high level of expression of such genes in leukemic blasts would thus be predictive of treatment failure.

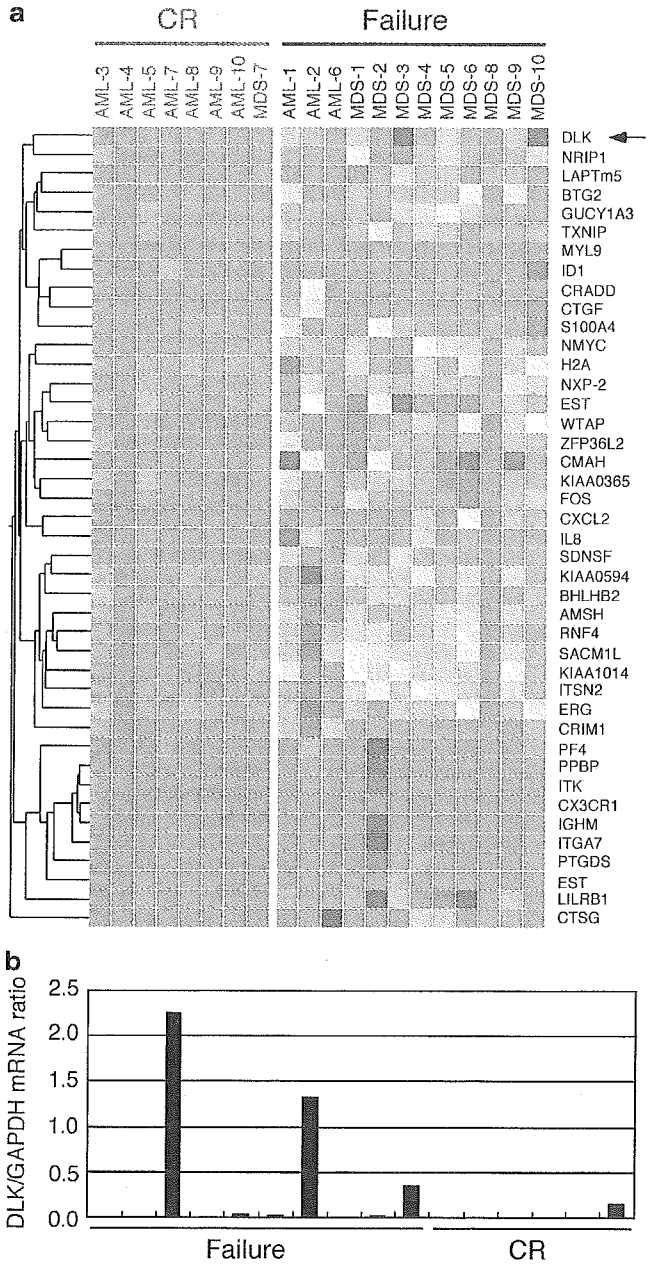

Figure 4 Identification of single gene markers for the prediction of chemoresistance. (a) Dendrogram showing the expression profiles of 42 genes whose expression intensity was <3.0 U in all CR samples and $\geqslant 10.0$ U in at least one sample in the Failure group. The row corresponding to DLK is indicated by an arrow. (b) Quantitation of DLK mRNA in AC133$^+$ blasts. The ratio of the abundance of the DLK mRNA to that of GAPDH mRNA was determined as in Figure 3b.

Among these genes was that for Delta-like (DLK),[16] a membrane protein that is thought to support the self-renewal of HSCs. With a cDNA microarray analysis of Blast Bank samples, we previously showed that *DLK* was transcriptionally active in the AC133$^+$ cells of individuals with MDS-related leukemia but not in those of patients with *de novo* AML.[11] Given the substantial overlap of the Failure group with the MDS-related AML group as well as the limited number of samples analyzed in the present study, it remains to be determined whether a high level of *DLK* expression is related to a specific disease type (MDS-related AML) or to chemosensitivity (treatment failure). However, independent analyses with distinct types of microarray (cDNA array and GeneChip) indicate that *DLK* is specifically activated in the blasts from individuals with overlapping subgroups of leukemia.

To confirm the GeneChip data, we determined the amount of *DLK* mRNA relative to that of *GAPDH* mRNA in the Blast Bank samples analyzed in the present study (Figure 4b). The relative abundance of *DLK* mRNA was significantly correlated with the expression intensity of *DLK* in the GeneChip analysis ($r=0.745$, $P=0.0016$).

Discussion

We have compared the gene expression profiles of AC133$^+$ cells from individuals with two distinct clinical courses of the M2 subtype of AML. Purification of the AC133$^+$ leukemic stem cells from these individuals allowed us to match the specimens as closely as possible prior to microarray analysis. Our study was thus designed to address the question of whether *de novo* AML is a distinct clinical entity from MDS-related AML, and, if so, how distinct?

The overall gene expression profiles did not clearly separate the samples into two major branches corresponding to *de novo* and MDS-related AML. However, two-way clustering analysis of the disease-associated genes resulted in separation of the samples into two groups that closely mirrored the clinical diagnosis. Many of the genes associated with MDS-related AML likely provide growth-promoting or antiapoptotic activities in the MDS blasts. The increased expression levels of genes encoding cyclins, molecules important for protein synthesis, and oncoproteins thus indicate that the proliferative potential of MDS blasts is greater than that of *de novo* AML blasts. A reduced expression level of the gene for the proapoptotic protein BAX[17] in the MDS blasts is also consistent with this notion. The relatively high accuracy of the prediction of clinical diagnosis on the basis of the expression profiles of the disease-associated genes suggests that the products of these genes may play important roles in the pathogenesis.

We also attempted to predict the clinical outcome of the first induction chemotherapy in our study subjects. The genes associated with chemoresistance included those for transcription factors or cofactors such as c-FOS, OZF, SP1, INT6, and ELE1, many of which are implicated in oncogenesis.[18–22] Furthermore, the outcome-associated genes included those for proteins, such as TOPIIB and RNA helicases (DDX17 and DDX3Y),[23] involved in the winding or unwinding of nucleotide strands. Altered expression of these proteins might be linked directly to resistance to certain types of anticancer drugs.

Finally, we attempted to identify single gene markers able to predict chemoresistance of leukemic blasts. Given that the

Failure group includes samples with different karyotypic anomalies, it might be expected that the mechanism of drug resistance of these samples exhibits similar heterogeneity. We therefore searched for genes that were silent transcriptionally in all samples of the CR group but were active in at least some of the samples in the Failure group.

Interestingly, out of the 42 'failure-specific' genes in Figure 4a, five genes encode for chemokines or chemokine receptors, such as proplatelet basic protein (GenBank accession number M54995) or CXC chemokine ligand 7, platelet factor 4 (M25897) or CXC chemokine ligand 4, interleukin 8 (IL8; M17017), chemokine CXC motif ligand 2 (M36820), and chemokine CX3C motif receptor 1 (U20350). Chemokines are a group of small proteins that play a pivotal role in the regulation of the immune system and of cell trafficking as well. Additionally, chemokines can exert pleiotropic effects on target cells, such as mitosis, homing, and even protection against chemotherapeutic reagents. A CC motif chemokine, CCL21, can inhibit, for instance, apoptosis induced by Ara-C.[24] Therefore, it would be possible that chemokine-mediated cell signaling helps to provide drug resistance to the leukemic blasts in our study. Given the high serum levels of IL8 protein in patients with AML and MDS,[25] activation of chemokine/chemokine receptor systems is likely to be relevant to the pathophysiology of leukemic disorders.

Certain types of transcriptional factors and/or their regulators are also activated transcriptionally in the drug-resistant leukemic blasts, including NMYC (GenBank accession number Y00664), basic helix–loop–helix domain containing class B2 (BHLHB2; AB004066), ID1 (X77956), ERG1 (M21535), and c-FOS. Additionally activated were the genes for nuclear proteins, that is, nuclear matrix protein NXP-2 (D50926), Wilms' tumor 1-associated protein 1 (WTAP; X84373), and nuclear receptor interacting protein 1 (NRIP1; X84373). NYMC, ERG1, and c-FOS all mediate mitotic signaling, and ID1 is known to inhibit cell differentiation. WTAP[26] and NRIP1[27] regulate the activity of WT1 and hormone receptors, respectively. Therefore, these gene products may be directly involved in the regulation of cell proliferation and differentiation process.

Conclusion

By narrowing the window of sample selection both to the same FAB subtype of *de novo* and MDS-related AML and to the same level of cell differentiation (as reflected by AC133 expression), we should have minimized population-shift effects that seriously hamper the ability to draw meaningful conclusions from microarray data. Further increases in the number of samples analyzed as well as in the number of genes on the arrays should help to pinpoint genes whose expression levels provide clinically useful information and make it possible to construct custom-made microarrays for the diagnosis of leukemias and the prediction of treatment outcome.

Acknowledgements

We thank all the physicians and patients who participated in the collection of Blast Bank samples. This work was supported in part by grants for Research on the Human Genome, Tissue Engineering, and Food Biotechnology, for the Second-Term Comprehensive 10-Year Strategy for Cancer Control, and for Research on Development of Novel Therapeutic Modalities for Myelodysplastic Syndrome from the Ministry of Health, Labor, and Welfare of Japan; by the Science Research Promotion Fund of the Promotion and Mutual Aid Corporation for Private Schools of Japan; by a grant from Research Foundation for Community Medicine of Japan; by a grant from Sankyo Foundation of Life Science; and by a grant from Takeda Science Foundation. JO is a research resident of the Japan Health Sciences Foundation.

References

1 Bennett JM, Catovsky D, Daniel MT, Flandrin G, Galton DAG, Gralnick HR *et al.* Proposals for the classification of the myelodysplastic syndromes. *Br J Haematol* 1982; **51**: 189–199.
2 Harris NL, Jaffe ES, Diebold J, Flandrin G, Muller-Hermelink HK, Vardiman J *et al.* World Health Organization classification of neoplastic diseases of the hematopoietic and lymphoid tissues: report of the Clinical Advisory Committee Meeting – Airlie House, Virginia, November 1997. *J Clin Oncol* 1999; **17**: 3835–3849.
3 Sole F, Espinet B, Sanz GF, Cervera J, Calasanz MJ, Luno E *et al.* Incidence, characterization and prognostic significance of chromosomal abnormalities in 640 patients with primary myelodysplastic syndromes. Grupo Cooperativo Espanol de Citogenetica Hematologica. *Br J Haematol* 2000; **108**: 346–356.
4 Greenberg P, Cox C, LeBeau MM, Fenaux P, Morel P, Sanz G *et al.* International scoring system for evaluating prognosis in myelodysplastic syndromes. *Blood* 1997; **89**: 2079–2088.
5 Bain BJ. The bone marrow aspirate of healthy subjects. *Br J Haematol* 1996; **94**: 206–209.
6 Kuriyama K, Tomonaga M, Matsuo T, Ginnai I, Ichimaru M. Diagnostic significance of detecting pseudo-Pelger–Huet anomalies and micro-megakaryocytes in myelodysplastic syndrome. *Br J Haematol* 1986; **63**: 665–669.
7 Jaffe ES, Harris NL, Stein H, Vardiman JW (eds). *Pathology and Genetics of Tumours of Haematopoietic and Lymphoid Tissues.* Lyon: IARC Press, 2001.
8 Duggan DJ, Bittner M, Chen Y, Meltzer P, Trent JM. Expression profiling using cDNA microarrays. *Nat Genet* 1999; **21**: 10–14.
9 Hin AH, Miraglia S, Zanjani ED, Almeida-Porada G, Ogawa M, Leary AG *et al.* AC133, a novel marker for human hematopoietic stem and progenitor cells. *Blood* 1997; **90**: 5002–5012.
10 Bennett JM, Catovsky D, Daniel MT, Flandrin G, Galton DA, Gralnick HR *et al.* Proposed revised criteria for the classification of acute myeloid leukemia. A report of the French–American–British Cooperative Group. *Ann Intern Med* 1985; **103**: 620–625.
11 Miyazato A, Ueno S, Ohmine K, Ueda M, Yoshida K, Yamashita Y *et al.* Identification of myelodysplastic syndrome-specific genes by DNA microarray analysis with purified hematopoietic stem cell fraction. *Blood* 2001; **98**: 422–427.
12 Ohmine K, Ota J, Ueda M, Ueno S-I, Yoshida K, Yamashita Y *et al.* on of stage progression in chronic myeloid leukemia by DNA microarray with purified hematopoietic stem cells. *Oncogene* 2001; **20**: 8249–8257.
13 Van Gelder RN, von Zastrow ME, Yool A, Dement WC, Barchas JD, Eberwine JH. Amplified RNA synthesized from limited quantities of heterogeneous cDNA. *Proc Natl Acad Sci USA* 1990; **87**: 1663–1667.
14 Alon U, Barkai N, Notterman DA, Gish K, Ybarra S, Mack D *et al.* Broad patterns of gene expression revealed by clustering analysis of tumor and normal colon tissues probed by oligonucleotide arrays. *Proc Natl Acad Sci USA* 1999; **96**: 6745–6750.
15 Valkov NI, Sullivan DM. Drug resistance to DNA topoisomerase I and II inhibitors in human leukemia, lymphoma, and multiple myeloma. *Semin Hematol* 1997; **34**: 48–62.
16 Moore KA, Pytowski B, Witte L, Hicklin D, Lemischka IR. Hematopoietic activity of a stromal cell transmembrane protein containing epidermal growth factor-like repeat motifs. *Proc Natl Acad Sci USA* 1997; **94**: 4011–4016.
17 Chou D, Miyashita T, Mohrenweiser HW, Ueki K, Kastury K, Druck T *et al.* The BAX gene maps to the glioma candidate region at 19q13.3, but is not altered in human gliomas. *Cancer Genet Cytogenet* 1996; **88**: 136–140.
18 Piechaczyk M, Blanchard JM, Marty L, Dani C, Panabieres F, Sabouty SE *et al.* Post-transcriptional regulation of glyceraldehyde-

3-phosphate-dehydrogenase gene expression in rat tissues. *Nucleic Acid Res* 1984; **12**: 6951–6963.
19 Ferbus D, Le Chalony C, Prosperi M-T, Muleris M, Vincent-Salomon A, Goubin G. Identification, nuclear localization, and binding activities of OZF, a human protein solely composed of zinc finger motifs. *Eur J Biochem* 1996; **236**: 991–995.
20 Yen H-CS, Gordon C, Chang EC. *Schizosaccharomyces pombe* Int6 and Ras homologs regulate cell division and mitotic fidelity via the proteosome. *Cell* 2003; **112**: 207–217.
21 Black AR, Black JD, Azizkhan-Clifford J. Sp1 and Kruppel-like factor family of transcription factors in cell growth regulation and cancer. *J Cell Physiol* 2001; **188**: 143–160.
22 Nikiforov YE, Koshoffer A, Nikiforova M, Stringer J, Fagin JA. Chromosomal breakpoint positions suggest a direct role for radiation in inducing illegitimate recombination between the ELE1 and RET genes in radiation-induced thyroid carcinomas. *Oncogene* 1999; **18**: 6330–6334.
23 Fouraux MA, Kolkman MJ, Van der Heijden A, De Jong AS, Van Venrooij WJ, Pruijn GJ. The human La (SS-B) autoantigen interacts with DDX15/hPrp43, a putative DEAH-box RNA helicase. *RNA* 2002; **8**: 1428–1443.
24 Hromas R, Cooper S, Broxmeyer HE. The chemokine CCL21 protects normal marrow progenitors from Ara-C cytotoxicity. *Cancer Chemother Pharmacol* 2002; **50**: 163–166.
25 Hsu HC, Lee YM, Tsai WH, Jiang ML, Ho CH, Ho CK *et al*. Circulating levels of thrombopoietic and inflammatory cytokines in patients with acute myeloblastic leukemia and myelodysplastic syndrome. *Oncology* 2002; **63**: 64–69.
26 Little NA, Hastie ND, Davies RC. Identification of WTAP, a novel Wilms' tumour 1-associating protein. *Hum Mol Genet* 2000; **9**: 2231–2239.
27 Cavailles V, Dauvois S, L'Horset F, Lopez G, Hoare S, Kushner PJ *et al*. Nuclear factor RIP140 modulates transcriptional activation by the estrogen receptor. *EMBO J* 1995; **14**: 3741–3751.

Cardiovascular Drugs and Therapy 17 231–236 2003

BASIC PHARMACOLOGY

Effects of Olmesartan, an Angiotensin II Receptor Blocker, on Mechanically-Modulated Genes in Cardiac Myocytes

Ruri Ohki[1], Keiji Yamamoto[1], Shuichi Ueno[1], Hiroyuki Mano[2], Uichi Ikeda[1], and Kazuyuki Shimada[1]

Divisions of [1]Cardiovascular Medicine and [2]Functional Genomics, Jichi Medical School, Minamikawachi-Machi, Tochigi, Japan 329-0498

Summary. Background: **Angiotensin II plays an important role in cardiac hypertrophy or remodeling. Angiotensin II receptor blockers (ARB) are clinically useful for the treatment of hypertension and heart failure. However, the molecular effects of ARB in the mechanically-stressed myocardium have not been completely defined. We investigated the effects of ARB on mechanically-modulated genes in cardiac myocytes.**

Methods: **We used powerful DNA microarray technology to study the effects of the ARB, CS-886 (olmesartan), on genes modulated in neonatal rat cardiac myocytes using mechanical stimuli. Mechanical deformation was applied to a thin and transparent membrane on which neonatal rat cardiac myocytes were cultured in the presence or absence of RNH-6270, an active metabolite of CS-886. Expression profiles of 8000 rat genes using the Affymetrix GeneChip (Rat Genome U34A) were investigated with mRNA obtained from the samples above.**

Results: **Nine genes induced under 4% mechanical strain were significantly suppressed by RNH-6270 in rat cardiac myocytes: monoamine oxidase B, neuromedine B receptor, olfactory receptor, synaptotagmin XI, retinol-binding protein, and 4 expressed sequence tags (ESTs). In contrast, 21 genes suppressed under mechanical strain were significantly restored by RNH-6270: major acute phase alpha 1-protein, Sp-1, Bcl-Xalpha, JAK2, 2 genes encoding detoxification, few genes for receptor, structure, metabolism or ion channel, and 10 ESTs.**

Conclusions: **As some of these genes may be involved in promoting or modulating cardiac remodeling, these findings suggest that ARB may affect cardiovascular morbidity and mortality partially via these molecular alterations.**

Key Words. **angiotensin II, mechanical, stress, gene expression, cardiac, myocyte**

Introduction

The renin-angiotensin system plays an important role in the regulation of blood pressure and fluid-electrolyte balance. The previous placebo-controlled trials such as CONSENSUS and SOLVD showed a significant benefit of angiotensin-converting enzyme (ACE) inhibitors in terms of morbidity and mortality in congestive heart failure [1,2]. In addition, treatment with ACE inhibitors attenuates left ventricular remodeling and improves prognosis in patients with significant left ventricular dysfunction after acute myocardial infarction [3]. ACE inhibitors, generally given with diuretics and digoxin, are the standard treatments for patients with heart failure and systolic left ventricular dysfunction. However, ACE inhibitors are associated with a variety of adverse events, cough being the most common [4].

An alternative approach to blockade of the renin-angiotensin system is the use of an angiotensin II type 1 receptor blocker (ARB). Since a new class of medication, ARB, has been developed to better block the vasoconstrictor-growth-promoting effects of angiotensin II directly at the receptor level [5], these drugs should provide similar benefits to ACE inhibitors in blocking the harmful effects of angiotensin II with fewer side effects. Recently, the Valsartan Heart Failure Trial (Val-HeFT) demonstrated that treatment with valsartan resulted in significant improvements in the New York Heart Association class, ejection fraction, signs and symptoms of heart failure, and quality of life as compared with placebo [6]. CS-866, olmesartan, is a new ARB that was first identified during a systemic survey of the angiotensin II type 1 receptor binding properties of substituted imidazole-5-carboxylic acids [7]. *In vivo*, CS-866 is rapidly and completely de-esterified to an active metabolite, RNH-6270, that is a highly selective antagonist of angiotensin II binding to the angiotensin II type 1 receptor [8].

With the recent discovery of the complete sequence of the human genome, new high-throughput approaches to studying these complex pathways have been made possible. In addition to identifying large clusters of genes that respond to a given stimulus, DNA microarray technology may be used to identify a few genes that comprise highly specific molecular responses [9]. Already, some studies using microarray technology have yielded interesting results regarding the pathogenesis

Address for correspondence: Keiji Yamamoto, MD, PhD, Division of Cardiovascular Medicine, Jichi Medical School, Minamikawachi-Machi, Tochigi, Japan 329-0498. Tel.: +81-285-58-7344; Fax: +81-285-44-5317; E-mail: kyamamoto@jichi.ac.jp

of cardiovascular diseases, such as myocardial infarction [10], cardiac hypertrophy [11], and human heart failure [12]. In the present study, using a DNA microarray and a mechanical deformation device that applies a highly uniform biaxial strain field to a culture substrate, we investigated the effects of ARB on genes modulated in neonatal rat cardiac myocytes with mechanical stimuli.

Methods

Materials

Fibronectin, bovine fetal calf serum (FCS) and Hanks' balanced salt solution (HBSS) were purchased from Life Technologies, Inc. (Rockville, MD). RNH-6270 was a gift from Sankyo Co., LTD. (Tokyo, Japan). All other chemicals used were of the highest grade commercially available.

Culture of neonatal rat ventricular myocytes (NRVM)

NRVM from 1-day old Sprague-Dawley rats were isolated by previously described methods [13]. The cells were cultured at 37°C, 5% CO_2 in Dulbecco's modified Eagle's medium (DMEM, BioWhittaker, Walkersville, MD) containing 7% FCS, 50 U/mL penicillin and 50 μg/mL streptomycin (PS).

This investigation was performed according to the *Guide for the Care and Use of Laboratory Animals* published by US National Institutes of Health (NIH publication No. 85-23, revised 1996).

Mechanical strain device and preparation of cells

Mechanical deformation was applied to a thin and transparent membrane on which cells were cultured, an approach which produces controlled cellular strain as well as visualization of cells [14]. For the preparation of NRVM to be subjected to mechanical strain, autoclaved membrane dishes were coated with 2 μg/mL of fibronectin in 13 mL of HBSS for 12 h at 4°C and then washed twice with 10 mL of PBS. NRVM were plated on the coated membrane dish at a density of 2,000,000 cells/dish in 13 mL of DMEM containing 7% FCS and incubated for 48 h. NRVM were then made quiescent by washing with 10 mL of HBSS twice and incubating with 10 mL of DMEM containing 1% insulin, transferrin, selenium media supplement (ITS; Sigma, St. Louis, MO) and PS. All experiments were performed on NRVM that had been serum-starved for 24 h.

Transcriptional profiling

NRVM cultured on fibronectin-coated membranes were harvested immediately after 6 h of cyclic deformation (1 Hz) or no deformation, and total RNA was extracted using RNeasy kit (QIAGEN K.K., Tokyo, Japan), and the purity was checked by spectrophotometry and agarose gel electrophoresis. Total RNA (20 μg) was converted to double-stranded cDNA using an oligo dT primer containing the T7 promoter (Gibco BRL Superscript® Choice System; Life Technologies, Inc.), and the template for an *in vitro* transcription reaction was used to synthesize biotin-labeled antisense cRNA (BioArray™ High Yield RNA Transcript Labeling Kit; Enzo Diagnostics, Farmingdale, NY). The biotinylated cRNA was fragmented and hybridized for 16 h at 45°C to GeneChip Test2 arrays (Affymetrix, Inc., Santa Clara, CA) to assess sample quality, and then to Rat Genome arrays (U34A, Affymetrix, Inc.). The arrays were washed, and then stained with streptavidin-phycoerythrin. The arrays were scanned with the GeneArray scanner (Agilent Technologies, Palo Alto, CA) and analyzed using the GeneSpring software package (Silicon Genetics, Redwood City, CA). Rat Genome U34A chip can detect 7,000 well-characterized genes with putative functions and 1,000 expressed sequence tags (ESTs).

Detailed protocols for data analysis of Affymetrix oligonucleotide microarrays and extensive documentation of the sensitivity and quantitative aspects of the method have been described [15]. Raw data from array scans were averaged across all gene probes for each array.

Real-time reverse transcription (RT)-PCR analysis

For RT, RNA was reverse transcribed using T7-dT primer (5′-TCT AGT CGA CGG CCA GTG AAT TGT AAT ACG ACT CAC TAT AGG GCG TTT TTT TTT TTT TTT TTT TTT-3′) and Superscript II reverse transcriptase (Life Technologies, Inc.). Real-time quantitative PCR was performed in optical tubes in a 96-well microtiter plate (Perkin-Elmer/Applied Biosystems, Foster City, CA) with an ABI PRISM 7700 Sequence Detector Systems (Perkin-Elmer/Applied Biosystems) according to the manufacturer's instructions. By using the SYBR Green PCR Core Reagents Kit (Perkin-Elmer/Applied Biosystems, P/N 4304886), fluorescence signals were generated during each PCR cycle via the 5′- to 3′-endonuclease activity of Taq Gold [16] to provide real-time quantitative PCR information. The primer set used for real-time PCR analysis contained the 5′-CATTGTGGCCTTCTTCTCCTT-3′ sense and 5′-TCCCGTAGAGATCCACAAAAGT-3′ antisense oligonucleotides for Bcl-Xalpha, 5′-GCCGTATGGAAGTTTACGAGAC-3′ sense and 5′-AGATCCCGGTGGATATACCTTT-3′ antisense oligonucleotides for JAK2 and 5′-TTCCAGTATGACTCTACCCACG-3′ sense and 5′-AGACTCCACGACATACTCAGCA-3′ for glyceraldehyde-3 phosphate dehydrogenase (GAPDH). No template controls as well as the samples were added in a total volume of 50 μL/reaction. Potential PCR product contamination was digested by uracil-N-glycosylase, because dTTP is substituted by dUTP [16]. All PCR experiments were performed with the hot start method. In the reaction system,

Table 1. Suppression of mechanically-induced genes by RNH-6270

GeneBank #	Description	Fold expression relative to control: Mechanical strain	Fold expression relative to control: Mechanical strain + RNH-6270
Metabolism			
M23601	Monoamine oxidase B	1.43 ± 0.04	1.15 ± 0.07
M10934	Retinol-binding protein	271.60 ± 19.51	140.92 ± 18.62
Receptors			
AF091575	Olfactory receptor	2.83 ± 0.07	1.99 ± 0.46
U37058	Neuromedin B receptor	24.77 ± 0.82	13.97 ± 4.19
Other			
AF000423	Synaptotagmin XI	3.38 ± 0.34	2.27 ± 0.28
ESTs			
AI639318		2.33 ± 0.08	1.00 ± 0.42
AI639100		3.94 ± 0.33	1.86 ± 0.88
AI639307		8.56 ± 1.61	2.94 ± 1.20
AA945585		9.25 ± 0.93	0.47 ± 0.20

Note: Values are mean ± SEM ($n = 3$). Nine mechanically-induced genes were significantly suppressed by RNH-6270 ($p < 0.05$).

uracil-N-glycosylase and Taq Gold (Perkin-Elmer/Applied Biosystems) were applied according to the manufacturer's instructions [16,17]. Denaturing and annealing reactions were performed 40 times at 95°C for 15 s, and at 60°C for 1 min, respectively. The increase in the fluorescence signal is proportional to the amount of specific product [18]. The intensity of emission signals in each sample was normalized to that of GAPDH as an internal control.

Statistical analysis

Data are expressed as the mean ± SEM. The data were analyzed by the nonparametric Kruskal-Wallis method to avoid assumptions about the distribution of the measured variables. Subsequent pairwise-comparisons were made with the Mann-Whitney U test; values of $p < 0.05$ were considered statistically significant.

Results

DNA microarray analysis of mechanically-modulated genes in cardiac myocytes

4% cyclic mechanical strain at 1 Hz in cultured rat cardiac myocytes significantly induced 45 genes (>2.0 fold, $p < 0.05$), including genes for heat shock protein 70, heme oxygenase, c-fos and adenosine A3 receptor, and 17 ESTs (available in an online only Data Supplement at http://www.kluweronline.com/issn/0920-3206). In contrast, 4% cyclic mechanical strain at 1 Hz in cultured rat cardiac myocytes significantly suppressed 94 genes (<0.5 fold, $p < 0.05$), including genes for cytochrome P450f, major acute phase alpha-1-protein and arylamine N-acetyltransferase, and 43 ESTs (available in an online only Data Supplement at http://www.kluweronline.com/issn/0920-3206).

DNA microarray analysis of suppression of mechanically-induced genes by RNH-6270 (Table 1)

Although the microarray hybridizations were performed three times, the results of these hybridizations regarding modulated genes were nearly identical. Of genes that were significantly induced under 4% cyclic mechanical strain at 1 Hz in cultured rat cardiac myocytes, we identified 9 genes that were significantly suppressed by RNH-6270 (0.1 μmol/L, $n = 3$, $p < 0.05$): monoamine oxidase B, retinol-binding protein, olfactory receptor, neuromedine B receptor, synaptotagmin XI, and 4 ESTs. There was suppression of genes encoding metabolism, monoamine oxidase B and retinol-binding protein, and receptors, olfactory receptor and neuromedine B receptor. It may be preferable that RNH-6270 significantly inhibited the mechanically-induced genes for monoamine oxidase B and neuromedine B receptor in rat cardiac myocytes, because monoamine oxidase B and neuromedine B are profoundly involved in catechol metabolism and mitosis or growth, respectively.

DNA microarray analysis of restoration of mechanically-suppressed genes by RNH-6270 (Table 2)

Next, we investigated whether mechanically-suppressed genes were restored by ARB. Of genes that were significantly suppressed under 4% cyclic mechanical strain in rat cardiac myocytes, we identified 21 genes that were significantly restored by RNH-6270 (0.1 μmol/L, $n = 3$, $p < 0.05$): Sp-1, Bcl-Xalpha, JAK2, neuritin, major acute phase alpha 1-protein, 2 genes encoding detoxification, few genes for receptor, structure, metabolism or ion channel, and 10 ESTs. Interestingly, RNH-6270, one of ARBs, restored the mechanically-suppressed genes for detoxification, cytochrome P-450f and arylamine N-acetyltransferase. In addition,

Table 2. Restoration of mechanically-suppressed genes by RNH-6270

GeneBank #	Description	Fold expression relative to control	
		Mechanical strain	Mechanical strain + RNH-6270
Transcription factor			
D12768	Sp-1	0.30 ± 0.18	0.90 ± 0.35
Detoxification			
M31031	CytochromeP-450f	0.15 ± 0.03	0.99 ± 0.21
U01344	Arylamine N-acetyltransferase	0.45 ± 0.16	0.88 ± 0.07
Humoral factor			
K02814	Major acute phase alpha 1-protein	0.35 ± 0.07	0.94 ± 0.31
Receptor			
M15682	Nicotinic acetylcholine receptor alpha subunit	0.10 ± 0.02	0.86 ± 0.30
Structure			
D26495	Dynein-like protein 4	0.10 ± 0.02	0.60 ± 0.20
Metabolism			
D26073	Phosphoribosylpyrophosphate synthetase-associated protein	0.38 ± 0.01	0.79 ± 0.03
Aitiapoptosis			
U72350	Bcl-Xalpha	0.33 ± 0.01	0.62 ± 0.10
Cell signaling			
U13396	JAK2	0.13 ± 0.06	0.55 ± 0.05
U88958	Neuritin	0.22 ± 0.08	0.51 ± 0.08
Channel			
M88751	Calcium channel beta subunit-III	0.11 ± 0.02	0.48 ± 0.02
ESTs			
AI178267		0.08 ± 0.02	0.77 ± 0.53
AI639401		0.10 ± 0.02	0.98 ± 0.36
AA893193		0.10 ± 0.03	0.33 ± 0.13
AA892754		0.14 ± 0.03	0.35 ± 0.06
AA894337		0.19 ± 0.08	0.35 ± 0.19
AI639146		0.20 ± 0.03	0.69 ± 0.24
AA891739		0.20 ± 0.02	0.94 ± 0.35
AI639162		0.28 ± 0.07	0.79 ± 0.04
AA799464		0.44 ± 0.03	0.91 ± 0.18
AA944973		0.54 ± 0.10	0.94 ± 0.12

Note: Values are mean ± SEM ($n = 3$). Twenty-one mechanically-suppressed genes were significantly restored by RNH-6270 ($p < 0.05$).

RNH-6270 restored the mechanically-suppressed gene expression for major acute phase alpha 1-protein of the rat that contains the sequence for bradykinin [19]. These findings suggest that ARB may provide much benefit in cardiovascular diseases, such as heart failure.

Real-time RT-PCR analysis

We confirmed expressions of two genes by real-time quantitative RT-PCR analysis. In real-time RT-PCR analysis, Bcl-Xalpha and JAK2 mRNA expressions were suppressed under 4% cyclic mechanical strain in rat cardiac myocytes (0.21 ± 0.01 fold and 0.21 ± 0.04 fold versus control, respectively, $n = 3$). These were significantly restored by RNH-6270 (0.38 ± 0.07 fold and 0.41 ± 0.06 fold versus control, respectively, $p < 0.05$).

Discussion

The present study using oligonucleotide microarray analysis demonstrates the changes in gene expression in stretch versus control neonatal rat cardiomyocytes and that nine genes induced under 4% mechanical strain, such as monoamine oxidase B and neuromedine B receptor were suppressed by RNH-6270 and that 21 genes suppressed under mechanical strain, such as genes for detoxification, cytochrome P-450f and arylamine N-acetyltransferase, and major acute phase alpha 1-protein were restored by RNH-6270. These molecular alterations might lead to the effects of ARB and a significant reduction in cardiovascular morbidity and mortality.

In the present study, nine genes induced under 4% mechanical strain were significantly suppressed by RNH-6270 in rat cardiac myocytes. Two of these genes encode the enzyme monoamine oxidase B and neuromedin B receptor. Human monoamine oxidase B plays a major role in the degradation of biogenic and dietary amines such as dopamine, thus increased myocardial degradation of dopamine may in part explain the deterioration of heart failure. In addition, the expression of neuromedin B receptor was also normalized by